Titre: Title:	Porosity dependence of mechanical properties of solid materials and rocks
Auteur: Author:	Qi Gu
Date:	2006
Type:	Mémoire ou thèse / Dissertation or Thesis
Référence: Citation:	Gu, Q. (2006). Porosity dependence of mechanical properties of solid materials and rocks [Mémoire de maîtrise, École Polytechnique de Montréal]. PolyPublie. https://publications.polymtl.ca/7624/

UNIVERSITÉ DE MONTRÉAL

ÉCOLE POLYTECHNIQUE DE MONTRÉAL

POROSITY DEPENDENCE OF MECHANICAL PROPERTIES OF SOLID MATERIALS AND ROCKS

QI GU

DÉPARTEMENT DES GÉNIES CIVIL, GÉOLOGIQUE ET DES MINES
ÉCOLE POLYTECHNIQUE DE MONTRÉAL

MÉMOIRE PRÉSENTÉ EN VUE DE L'OBTENTION
DU DIPLÔME DE MAÎTRISE ÈS SCIENCES APPLIQUÉES
(GÉNIE MINÉRAL)

FÉVRIER 2006

Your file Votre référence
ISBN: 978-0-494-16792-2
Our file Notre référence
ISBN: 978-0-494-16792-2

UNIVERSITÉ DE MONTRÉAL

ÉCOLE POLYTECHNIQUE DE MONTRÉAL

Ce mémoire intitulé

POROSITY DEPENDENCE OF MECHANICAL PROPERTIES OF SOLID MATERIALS AND ROCKS

présenté par: GU Qi

en vue de l'obtention du diplôme de: Maîtrise ès sciences appliquées

a été dûment accepté par le jury d'examen constitué de:

M. CHOUTEAU Michel, Ph.D., président

M. JI Shaocheng, Ph.D., directeur de recherche

M. MARTIGNOLE Jacques, D.Sc., membre

Acknowledgments

I express my extreme sense of gratitude to my research supervisor Professor Shaocheng Ji, Department of Civil, Geological and Mining Engineering, École Polytechnique de Montréal, for his guidance, stimulating discussion, intellectual, inspiration, encouragement, sound advice and good teaching during this study.

Résumé

Les moyennes généralisées sont employées comme règle de mélange simple mais élégante pour fournir une description unifiée des propriétés physiques des composites polyphasés en termes de propriétés des composants, des fractions volumique, et des microstructures. Cette formule est appelée règle généralisée de mélange (GMR: 'generalized mixture rule'). En prenant les matériaux poreux comme une classe spéciale de composites biphasés dans lesquels des pores sont dispersés dans un milieu solide, le GMR rapporte une expression rigoureuse pour la dépendance des propriétés mécaniques en fonction de la porosité. Bien que le GMR soit d'origine purement mathématique, son lien avec des théories existantes et sa cohérence avec une grande quantité de données expérimentales suggèrent qu'il devrait avoir une certaine validité physique ou au moins comme outil très pratique pour décrire les propriétés mécaniques des matériaux multiphasés incluant les solides poreux. On suggère que le GMR devrait être largement utilisé pour modeler la résistance l'écoulement des roches polyminérales déformées sous divers états physiques et chimiques (température, pression, taux et type de déformation et teneur en eau) dan la lithosphère.

Abstract

The generalized means are used as a simple but elegant mixture rule for providing a unified description of the physical properties of polyphase composites in terms of component properties, volume fractions, and microstructures. This formula is named as the generalized mixture rule (GMR). Taking porous materials as a special class of two-phase composites in which pores are dispersed within a solid framework, the GMR yields a rigorous expression for the porosity dependence of the mechanical properties. Although the GMR is purely mathematical in origin, its connection to the existing theories and its consistence with extensive experimental data suggest that it should have some physical validity as a hypothesis or at least a very handy tool for a general description of the mechanical properties of multiphase materials including porous solids. It is suggested that the GMR should be widely used to modeling the flow strengths of polymineralic rocks deformed under various physical and chemical conditions (e.g., temperature, pressure, strain rate and water content) in the lithosphere.

Condensé en français

0.1. Introduction

La modélisation des propriétés mécaniques des composites est impliquée dans l'utilisation des règles appropriées de mélange. En fait, certaines des règles importantes peuvent être unifiées par une règle généralisée de mélange (GMR : 'generalized mixture rule') exprimée comme (Ji, 2004a and b):

$$M_c^{\ J} = \sum_{i=1}^{N} \left(V_i M_i^{\ J} \right) \qquad (1)$$

M est une propriété spécifique (par exemple, module de Young, résistance d'écoulement plastique), J est une constante, V est la fraction de volume du composant, les indices inférieurs i et c représentent, respectivement, la phase d'i^e et le composite se composant de N phases,

$$\sum_{i=1}^{N} V_i = 1 \qquad (2)$$

0.2. Les caractéristiques de GMR

Des microstructures sont exprimées par un paramètre fractal J, qui est principalement commandé par la forme, la distribution de tailles de grains, et la distribution spatiale (continuité et connectivité) des phases (Ji, 2004a and b). $M_c(J)$ a les caractéristiques suivantes :

(a) $M_c(J)$ est une fonction croissante continue et monotone pour toutes les valeurs de J dans les gammes $(-\infty \le J \le \infty)$. Cette monotonie est valable en ce qui concerne les fractions de volume ou les propriétés physiques.

(b) Pour $J<1$, $J=1$ et $J>1$, $M_c(J)$ en fonction des différentes catégories de variables est fortement concave, linéaire, et fortement convexe, respectivement.

(c) Pour un système binaire qui se compose d'une phase forte (s) et d'une phase faible (w), $J<0$ pour la structure soutenue par la phase faible (Ji, 2004a and b), et $J>0$ pour la structure soutenue par la phase forte (Ji, 2004a and b). Le GMR satisfait les conditions limites suivantes: pour $V_s=0$ (agrégat pur de phase faible), les propriétés effectives sont équivalentes aux propriétés de la phase faible pour toutes les valeurs de J. De même, pour $V_s=1$ (agrégat pur de phase forte), les propriétés effectives sont équivalentes aux propriétés de la phase forte pour toutes les valeurs de J. Dans la circonstance telle que $M_s=M_w$ (deux phases ont une propriété équivalente), puis $M_c=M_s=M_w$ pour toutes les valeurs de J et toutes les valeurs de V_s.

(d) Le cas $J=1$ rapporte la moyenne arithmétique ou la moyenne de Voigt (qui assument la contrainte constante). Le cas $J=-1$ rapporte la moyenne harmonique ou celle de Reuss (qui assument la déformation constante). Pour les composites isotropes, les moyennes de Voigt et de Reuss sont généralement considérées comme les limites supérieures et inférieures pour les propriétés élastiques effectives (Hill, 1965). Pour un composite se composant des particules rigides dans une matrice débordante équilibrée, cependant, sa résistance de fluage peut être inférieure au Reuss si l'exposant J de la matrice est suffisamment grand, par exemple, >4. Le GMR avec $J\rightarrow 0$ rapporte le moyenne géométrique. Le dernier devient physiquement sans signification quand une des phases constitutives a une propriété nulle. Dans ce cas spécial, la propriété globale du composite acquis de la moyenne géométrique disparaîtra toujours indépendamment de la fraction de volume du constituant qui a une propriété nulle.

0.3. Applications de GMR

Le GMR avec $J \to 0$ rapporte la moyenne géométrique. Ji et al. (2004) ont constaté que le GMR avec J=0.5 et J==-0.5 fournit à la bonne concordance les données expérimentales du module de Young pour les composites biphasés dans lesquels des inclusions sont formées comme des sphères d'isolement dans des médias continus, plus forts et plus faibles, respectivement. Pour la plupart des composites dans lesquels les inclusions ont une géométrie plus ou moins arbitraire, le GMR avec J=-0.25 et J=0.25 prévoit les valeurs mesurées du module de Young pour ceux avec une structure soutenue par la phase faible ($V_s \leq 0.5$) et pour ceux avec une structure soutenue par phase forte ($V_s \geq 0.7$), respectivement. Dans le domaine intermédiaire ($0.5 \leq V_s \leq 0.7$), J s'est avéré changer progressivement de -0.5 à 0.5 ou de -0.25 à 0.25 à cause de la transition dans la microstructure.

Récemment, Ji (2004) a prouvé que diverses expressions célébres telles que l'équation d'Einstein pour les suspensions idéales et diluées (Einstein, 1906) et la formule de Roscoe (1952) pour les suspensions générales de solide-liquide peuvent être dérivées en tant que cas spéciaux du GMR en utilisant le paramètre microstructural J=-0.4. Il a été démontré que le GMR fonctionne bien pour décrire les diverses propriétés mécaniques (par exemple, modules élastiques, dureté, résistance à l'écoulement) pour les éventails de systèmes multiphasés allant des roches naturelles à la céramique et aux alliages industriels.

0.4. Analyse de GMR

Pour un composite biphasé, Eq. (1) peut être simplifié :

$$M_c^{\ J} = (1 - V_w) M_s^{\ J} + V_w M_w^{\ J} \qquad (3)$$

Les matériaux poreux sont considérés comme une classe spéciale de composites biphasés dans lesquels les pores avec résistance nulle (i.e., M_w=0) sont dispersés dans un milieu solide. Soit V_w et une porosité (p), on peut évaluer l'effet de la porosité sur la propriété. Eq. (3) peut être écrit de la façon suivante

$$\frac{M_c}{M_s} = (1-p)^{1/J} = V_s^{1/J} = \left(\frac{\rho_c}{\rho_s}\right)^{1/J} \qquad (4)$$

J est le paramètre qui dépend de la forme géométrique, de la distribution spatiale d'arrangement, de l'orientation et de la dimension des pores, et alternativement des matériaux et de la méthode de fabrication (i.e., pression à froid, agglomération, ou pression isostatique chaude) ; ρ_c et ρ_s sont les densités des matériaux poreux et non-poreux, respectivement; ρ_c/ρ_s est la densité relative qui égale la masse de fraction de volume. Sur les échelles de $\log(M_c/M_s)$ par $\log(1\text{-}p)$ ou $\log(\rho_c/\rho_s)$, $1/J$ est la pente de la dépendance de la propriété sur la gamme linéaire. La valeur de J devrait se situer dans la gamme de 0 à 1, donnant un éventail de propriétés à une densité relative ou à une porosité indiquée. La variation de J avec la microstructure apporte une grande possibilité pour optimiser les propriétés mécaniques des solides poreux. De plus, la porosité a un plus grand effet sur les propriétés mécaniques à de plus petites valeurs de J.

J=1 pour les matériaux poreux avec pores cylindrique ou hexagonaux parallèles à la direction d'effort,

$$\frac{M_c}{M_s} = 1 - p = \frac{\rho_c}{\rho_s} \qquad (5)$$

Eq. (5) apporte un rapport linéaire entre M_c/M_s et p, et la bonne concordance avec des résultats expérimentaux du lotus-type métaux poreux avec les longs pores parallèles à la direction de chargement (Hyun et al., 2001; Ichitusubo et al., 2002), Généralement, les pores de canal intergranulaires, et continus correspondent à une valeur plus basse de J que les pores intragranulaires, d'isolement et arrondis. Les pores ouverts montrent une valeur plus basse de J et des effets plus prononcés sur les propriétés mécaniques effectives que les pores fermés. Ainsi, la dépendance complexe de J à l'égard de la microstructure est un sujet crucial pour l'étude afin de mieux prévoir et d'optimiser les propriétés mécaniques des solides poreux.

Eq. (4) peut être étendue à une série entière :

$$\frac{M_c}{M_s}=1+\left(-\frac{1}{J}p\right)+\frac{\frac{1}{J}\left(\frac{1}{J}-1\right)}{2}p^2+\frac{\left(-\frac{1}{J}\right)\left(\frac{1}{J}-1\right)\left(\frac{1}{J}-2\right)}{6}p^3+\cdots\cdots \qquad (6)$$

Pour des valeurs basses de porosité (p<<1), Eq. (6) peut être raisonnablement approchée par

$$\frac{M_c}{M_s}=1-\frac{1}{J}p \qquad (7)$$

Eq. (7) indique une relation linéaire entre M_c/M_s et p à de basses porosités (p< 0.10-0.15).

La forme de pore, ce qui est l'un des facteurs les plus importants pour affecter la valeur de J, peut être caractérisé par le facteur de forme (S) qui est défini ci-dessous :

$$S=4\pi A/L^2 \qquad (8)$$

A est l'aire de la section des pores et L est le périmètre des pores dans une lame-mince sectionnée aléatoirement. A et L peuvent être mesurés en utilisant l'analyse d'image quantitative. S diminue dans la grandeur pendant que le contour des pores devient plus irrégulier. Par exemple, S=1 pour un cercle parfait, S=0.785 pour un carré, S=0.604 pour un triangle équilatéral, et S tend vers zéro si la forme des pores devient une ligne (Russ, 1986). Les pores sphériques se produisent généralement à basse porosité. À mesure que la porosité augmente, le facteur de forme diminue et la géométrie des pores devient de plus en plus plus complexe. Quand la porosité est plus haute qu'une valeur critique (p_{c1}), les pores deviennent de plus en plus plus ouverts (Nielsen, 1982). D'ailleurs, les grands pores sont généralement plus irréguliers que de petits pores, indiquant que les grands pores peuvent se former à partir de l'agglomération de petits pores. En conséquence, les diminutions de valeur de S (Beiss et al., 2001) et donc ainsi la valeur de J avec l'augmentation de la taille des pores. Réciproquement, une tendance à diminuer de S avec la taille décroissante des pores peut se produire si de petits pores irréguliers étaient produits par fragmentation de grands pores. Ainsi, la valeur de J peut refléter les processus de formation des matériaux.

En outre, les propriétés mécaniques d'un matériel non-poreux peuvent être estimées à partir de ses contre-parties poreuses selon l'équation suivante :

$$M_s = \left[\frac{M_c^{\ J}}{1-\phi}\right]^{1/J} \qquad (9)$$

Pour un but d'inversion, une formule analytique telle que Eq. (9) est avantageux que des codes informatiques compliqués et pénibles.

0.5. Conclusions

(1) Le GMR ('generalized mixture rule') est une formule mathématique rigoureuse à symétrie simple. Il ne postule aucune prétention sur les propriétés physiques, les processus, ou les microstructures. Ainsi, il est raisonnable de croire que le GMR reflète la nature aléatoire de la microstructure dans les matériaux polyphasés.

(2) Le GMR fournit une description unifiée pour le meilleur rapport convenable entre les propriétés mécaniques globales (par exemple, constantes élastiques, résistances d'écoulement plastique), la fraction de volume, et la microstructure de chaque composant dans les composites multiphasés. Pour les solides poreux, les diverses équations bien connues telles que loi de Balshin (1949), l'équation exponentielle de Duckworth (1951), la formule de Gibson-Ashby (1988), et l'expression de Phani (1986) sur le rapport entre les propriétés mécaniques et la porosité peuvent être dérivées directement du GMR. Pour des porosités < 30%, le GMR est conforme aux résultats des modèles théoriques précédents basés sur quelques structures uniformes idéal (par exemple, Eudier, Ramakrishnan et Arunachalam, Ishai et Cohen, et autres) dans les limites d'erreur au plus de quelques pourcent. De plus, l'accord entre le GMR et les données expérimentales sur les éventails de systèmes polyphasés comprenant les solides poreux ne peut pas être considéré comme fortuit. Le GMR devrait avoir une validité physique et théorique ou au moins hypothètique et constitue un outil phénoménologique pour une description générale des propriétés mécaniques des matériaux multiphasés incluant les solides poreux. Des analyses théoriques rigoureuses sont nécessaires parce que la signification physique fondamentale du GMR n'est pas claire. Ainsi le travail actuel fournit une base pour de futures études.

(3) L'exposant caractéristique J du GMR fournit un paramètre d'ajustement pour décrire quantitativement les effets des microstructures complexes sur les propriétés

physiques globales. Ce paramètre, qui est appelé coefficient microstructural, est commandé principalement par la forme, la distribution de grandeurs dimensionnelles, la continuité et la connectivité des phases, et peut refléter les processus de formation des matériaux. Ainsi, la valeur de J peut être employée pour classifier les matériaux polyphasés. Pour les matériaux poreux type-lotus avec de longs pores cylindriques ou hexagonaux, orientés parallèlement et perpendiculairement à la direction d'effort, J=1 et J=1/3, respectivement. Pour $J \rightarrow 0$ (la moyenne géométrique), équivalent à la limite inférieure de Hashin-Shtrikman (1963) dans le cas des matériaux poreux, on a un cas extrême où la propriété efficace d'un matériel poreux disparaîtra, indépendamment de la porosité. Pour J=~0.50 pour les matériaux poreux dans lesquels des pores parfaitement sphériques et isolés sont aléatoirement distribués dans une matrice solide continue. Pour le module de Young, J=~0.25 pour les matériaux polycristallins contenant des pores intergranulaires. La présence de pores elliptiques plats aura comme conséquence une plus petite valeur de J. Généralement, les pores de canal intergranulaire et continu causent une valeur plus basse de J que les pores intragranulaires d'isolement et arrondis. Par conséquent, l'arrondissage et le débranchement des pores devraient avoir comme conséquence une augmentation des propriétés mécaniques effectives des matériaux avec une porosité constante. En d'autres termes, l'optimisation des propriétés mécaniques des matériaux peut être faite en présentant différentes fractions de volume et/ou différentes formes des pores dans les solides. Une conclusion additionnelle est que les valeurs de J pour les modules du cisaillement, de Young, et d'incompressibilité, et le rapport de Poisson peuvent ne pas être identiques même pour un matériel poreux avec une microstructure constante. Par conséquent, il y a un besoin de recherche à ce sujet.

(4) L'application du GMR pour prévoir les propriétés mécaniques des matériaux polyphasés est plus direct comparé à d'autres approches telles que les limites supérieures et inférieures de Hashin-Shtrikman (1963). Dans le cas de l'élasticité, le GMR n'a pas besoin de connaître les modules de compressibilité et de cisaillement séparément.

Cependant, les calculs des limites de Hashin-Shtrikman (1963) exigent des informations complètes sur les modules de compressibilité et de cisaillement pour chaque phase des matériaux. Un ensemble complet des données élastiques manque habituellement parce que seule une propriété élastique est le plus souvent mesurée. Dans ces derniers cas, les limites de Hashin-Shtrikman (1963) ne peuvent pas être calculées. Pour les matériaux poreux, les limites supérieures et inférieures de Hashin-Shtrikman se trouvent trop loin à part pour être utiles dans la prévision des propriétés élastiques en fonction de la porosité parce que les pores ont une résistance nulle et la limite inférieure de Hashin-Shtrikman est toujours zéro pour tous les modules indépendamment de la porosité.

(5) Le GMR, comparé à beaucoup de méthodes numériques compliquées qui sont utilises pour chaque composite, a l'avantage d'avoir une formule analytique plutôt qu'informatique. Cet avantage est extrêmement utile si on désire inverser les données mécaniques d'un composite pour calibrer la microstructure ou pour estimer la propriété ou la fraction de volume d'un constituant pur du composite.

Table of contents

ACKNOWLEDGMENTS IV

RÉSUMÉ V

ABSTRACT VI

CONDENSÉ EN FRANÇAIS VII

TABLE OF CONTENTS XVI

LIST OF FIGURES XVII

LIST OF TABLES XVII

LIST OF SYMBOLS XXI

CHAPTER 1 INTRODUCTION 1

CHAPTER 2 GENERALIZED MIXTURE RULE (GMR) 7

2.1. Description of the generalized mixture rule (GMR) 7

2.1.1. Introduction 7

2.1.2. Characteristics of GMR 7

2.1.3. Applications of GMR 9

2.2. Analysis of GMR 10

2.3 Comparison of GMR with other expressions 13

CHAPTER 3 COMPARISON WITH EXPERIMENTS 31

CHAPTER 4 CONCLUSIONS 54

REFERENCES 57

List of figures

Figure 2.1 Relative tensile strengths of lotus-type porous cooper as a function of porosity. Theoretical curves labeled according to J values. 12

Figure 2.2 Histograms of J values for the Young's modulus (a) and shear modulus (b) of polycrystalline aggregates. Data mainly from R.W. Rice (1998). N, the number of measurements; J_{Me}, the median (the fiftieth percentile in the distribution). 24

Figure 2.3 Comparison of the GMR with the theoretical models of Eudier (1962). 26

Figure 2.4 Comparison of the GMR with the theoretical models of Ramakrishnan and Arunachalam (1990). 28

Figure 2.5 Relative mechanical properties of solids containing cubic pores with their <100> (a), <110> (b) and <111> (c) directions parallel to the loading direction 29

Figure 3.1 Comparison of the theoretical values calculated from the GMR with experimental data on relative Young's modulus of porous material Al_2O_3 (Knudson, 1962). 33

Figure 3.2 Comparison of the theoretical values calculated from the GMR with experimental data on relative Young's modulus of porous material Al_2O_3 (Spriggs, 1961). 34

Figure 3.3 Comparison of the theoretical values calculated from the GMR with experimental data on relative Young's modulus of porous material MgO (Spriggs, 1962). 35

Figure 3.4 Comparison of the theoretical values calculated from the GMR with experimental data on relative Young's modulus of porous material SiC (Reynaud et al., 2005). 35

Figure 3.5 Comparison of the theoretical values calculated from the GMR with experimental data on relative Young's modulus of porous material $MgAl_2O_4$ (Porter et al., 1977). 36

Figure 3.6 Comparison of the theoretical values calculated from the GMR with experimental data on relative shear modulus of porous material $MgAl_2O_4$(Porter et al., 1977). 37
Figure 3.7 Comparison between experimental and theoretical results for relative Young's modulus of phosphate-bonded, alumina filled magnesia ceramics. 38
Figure 3.8 Comparison between experimental and theoretical results for relative Young's modulus for sandstone analogs made from fused glass beads. Theoretical curves labeled according to J value. HS+ represents the Hashin-Shtrikman upper bound. 41
Figure 3.9 Comparison between experimental and theoretical results for relative shear modulus for sandstone analogs made from fused glass beads. Theoretical curves labeled according to J value. HS+ represents the Hashin-Shtrikman upper bound 42
Figure 3.10 Comparison between experimental and theoretical results for relative bulk modulus for glass foams..... 43
Figure 3.11 Comparison between experimental and theoretical results for relative yield strength of porous epoxy. 44
Figure 3.12 Comparison between experimental and theoretical results for relative compressive strengths for Cu/Cu_2O cermets. 45
Figure 3.13 Relative ductile strength for Fe aggregates plotted against porosity. 47
Figure 3.14 Relative ductile strength for sintered steels plotted against porosity..... 48
Figure 3.15 Relative ductile strength for Fe-Cu alloys plotted against porosity..... 49
Figure 3.16 Relative ductile strength for sintered Cu, Ni and Fe plotted against porosity. 50
Figure 3.17 Relative ductile strength for sintered Al plotted against porosity. 51
Figure 3.18 Relative elastic properties (E, G, K, υ, V_p and V_s) for titanium aluminide (Ti-24Al-11Nb) compacts plotted against porosity. 52

Figure 3.19 P-wave and S-wave velocities (km/s) in water-saturated basalts plotted against porosity. 53

List of tables

Table 2.1 The *J* values obtained by fitting the GMR with experimental results for Young's modulus of various materials..... 19

Table 2.2 The J values obtained by fitting the GMR with experimental results usingthe least squares regression analysis for shear moduli (G) of polycrystalline aggregates..... 23

List of symbols

M	Specific property
E	Young's modulus
G	Shear modulus
K	Bulk modulus
σ_y	Yield strength
σ_r	Rupture strength
σ_f	Flow strength
V	Volume fraction of a component
J	Microstructural parameter
ϕ	Volume fraction of hard particles
ρ_c	Density of a porous material
ρ_s	Density of a nonporous material
p_c	Critical porosity above which the stress-supporting solid framework fails
L	Pore perimeter
A	Solid area of a porous material normal to the reference direction
A_0	Solid area of a porosity-free material normal to the reference direction
υ	Poisson's ratio

Chapter 1. Introduction

Porosity is an important microstructural feature in most natural and man-made materials and often affects significantly the physical properties of these materials. Typical examples of natural porous materials are sediments (e.g., soils, sands and sandstone), and basalts (volcanic rocks). A better knowledge of the porosity-dependence of rock mechanical properties is required to anticipate and minimize the technical problems in oil reservoirs such as earth surface subsidence and well-bore instability. Biological materials such as woods and bones are equally porous materials. Man-made porous materials such as foamed metals, sintered ceramics, hollow concretes and cellular polymers are widely used for thermal and acoustic insulation, impact energy absorption, vibration suppression, air or water filtration, fluid flow control, self-lubricating bearing, floatation and lightweight components. Further, traditional construction materials such as bricks, tiles, cements and concretes all are porous. Thus, to model accurately the mechanical properties of candidate solid materials in terms of their component properties, porosity and microstructure has broad significance for a wide range of fields from materials engineering to Earth sciences.

Despite the obvious importance of porosity as mentioned above, much is still not well known including how quantitatively the properties depend on porosity and pore geometry. Some properties (e.g., molecular weight and lattice parameter) have little or no obvious dependence on porosity, mainly those determined primarily or only by the chemical composition and atomic bonding or both. In contrast, other properties depend primarily or solely on the amount of porosity (p). In other words, these properties satisfy a rule of mixtures of the volume fractions of pore (p) and solid phases ($1-p$). Such properties include fluid permeability, thermal conductivity, electrical conductivity,

dielectric constant, magnetic permeability, diffusion coefficient, acoustic wave velocities, elastic moduli, and yield, rupture or ductile strength.

The relationship between porosity and mechanical properties of porous materials has received extensive studies during the last 6 decades. Detailed review and discussion of the available literature is outside the scope of the present thesis and can be found elsewhere (e.g., Allen, 1984; Rogers et al., 1994; Rice, 1998; Gibson and Ashby, 1999; Torquato, 2002). For simplicity, a brief review is given to some commonly used expressions for the effects of porosity on the mechanical properties of materials.

The relation between Young's modulus and porosity usually takes the form of an exponential expression:

$$E(p) = E_0 \exp(-bp) \qquad (1.1)$$

where $E(p)$ is the Young's modulus of a given material with porosity p, E_0 is the corresponding Young's modulus for zero porosity, and b is an empirical constant related to the type of material and to its pore geometry such as pore size, shape and distribution. Plotting $\ln E$ against p gives a linear correlation. Similarly, bulk and shear moduli (K and G) can be correlated with porosity. Equation 1.1 was proposed for the first time by Duckworth (1951), and since then it has been widely used as an empirical equation to predict the effective Young's modulus of porous materials. Equation (1.1) is considered to be valid when $p \leq 50\%$. A similar expression,

$$\sigma(p) = \sigma_0 \exp(-kp) \qquad (1.2)$$

was suggested for the relation between porosity and mechanical strength (σ). The latter can be taken as the yield strength (σ_y), rupture strength (σ_r) or ductile flow strength (σ_f). However, the application of Equations (1.1-1.2) is criticized for two major reasons: (i)

They were derived on a purely empirical basis without understanding physical meaning; and (ii) They do not satisfy the boundary condition of E=0 (or σ=0) for p=1 (Hasselman, 1962).

Spriggs (1961) proposed an empirical expression:

$$E(p) = E_0\left[1 + \frac{Ap}{1-(A+1)p}\right] \tag{1.3}$$

where A is an adjustable parameter. Clearly, this equation satisfies the boundary condition $E(p)$=0 when p=1 for whatever the A value is.

The most popular empirical equation is probably that proposed by Balshin (1949):

$$E(p) = E_0(1-p)^m \tag{1.4}$$

where m is a constant whose physical meaning is not yet understood. Equations (1.1) through (1.4) all are empirical and have been typically used to fit to experimental data plots using standard statistical techniques. A minimal standard error of estimate is generally cited for selecting one functional expression over another. Scatter in data plots is usually attributed to variations in shape, size, and spatial distribution of pores or simply to experimental errors.

An expression was also proposed by Hasselman (1962) based on the theory of Hashin (1962):

$$E(p) = E_0\left[1 - \frac{Bp}{1-(B+1)p}\right] \tag{1.5}$$

where B is an adjustable parameter.

A set of analytical equations has been proposed on the basis of the theory of elasticity of a continuum in which pores are a second phase dispersed homogeneously in a continuous solid media. Using the energy theorems of elasticity theory, Paul (1960) derived the following equation for the porous materials containing idealized cubic shaped, non-interconnected pores:

$$E(p) = E_0 \frac{1-p^{2/3}}{1-p^{2/3}\left(1-p^{1/3}\right)} \tag{1.6}$$

Phani and Niyogi (1987) derived an equation for the porosity dependence of the elastic modulus by assuming that the physical processes such as stress distribution is dependent only on total porosity; thus, the elastic modulus depends only on the total porosity. The equation proposed by Phani and Niyogi (1987) is:

$$E(p) = E_0(1-ap)^n \tag{1.7}$$

where a is related to the packing density and equals the inverse of the corresponding critical porosity (p_c) above which the elastic modulus vanishes. That is,

$$a = \frac{1}{p_c} \tag{1.8}$$

The definition implies that a is always greater than 1 unless p_c=1. However, the curves of experimental data over a wide range of porosity invariably give that a = 1 (Phani, 1986; Phani and Niyogi, 1987). Thus, Eq. (1.7) cannot explain the experimental data accurately unless a=1. In addition, the approach taken by Phani and Niyogi (1987) does not involve microstructures of the material such as the random shapes and size distribution of the pores. Hence the theory cannot be extended to more general applications in porous materials mechanics such as the dependence of elastic strength on pore shape and size.

Considering a solid cube of unit volume containing a spherical hole, Eudier (1962) obtained

$$E(p) = E_0\left[1-\pi\left(\frac{3}{4\pi}\right)^{2/3} p^{2/3}\right] = E_0\left(1-1.21p^{2/3}\right) \tag{1.9}$$

Equation (1.9) is valid only when $p<\pi/6$ or 0.524.

Assuming a cubic shape of pores embedded in a continuum matrix, Ishai and Cohen (1968) derived the following relation:

$$E(p) = E_0\left(1-p^{2/3}\right) \tag{1.10}$$

The Young's modulus calculated from this equation is the value along the reference direction parallel to the <100> directions of the pores. For the reference directions parallel to the <110> and <111> directions of the pores,

$$E(p) = E_0\left(1-\sqrt{2}p^{2/3}\right) \tag{1.11}$$

and

$$E(p) = E_0\left(1-\sqrt{3}p^{2/3}\right) \tag{1.12},$$

respectively (Rice, 1998). Thus, a solid material containing uniformly aligned cubic pores should be elastically or seismically anisotropic with the maximum and minimum moduli in the directions parallel to the <100> and <111> directions of pores, respectively.

Bert (1985) critically reviewed the equations derived by assuming regular shapes and arrangements of pores and concluded that the equations have limited applications. Therefore, there is indeed a need for a generalized model that can describe the porosity dependence of mechanical properties of porous materials by retaining a random structure. Such a model should contain a flexible parameter to describe the details of the microstructure of a porous material, i.e., the irregular shapes and varied sizes of the pores and their random distribution. This yields the purpose of the present study. It is involved to apply the generalized mixture rule (GMR) proposed by Ji (2004) for predicting the mechanical properties of porous materials.

Chapter 2. Generalized Mixture Rule (GMR)

2.1. Description of the generalized mixture rule (GMR)

2.1.1. Introduction

The modeling of composite mechanical properties is involved in the utilization of appropriate mixture rules. Actually some of the important rules can be unified by a generalized mixture rule (GMR) expressed as:

$$M_c^J = \sum_{i=1}^{N} \left(V_i M_i^J \right) \qquad (2.1)$$

where M is a specific property (e.g., Young's modulus, yield strength or ductile flow strength), J is a microstructural parameter, V is the volume fraction of constituent component, the subscripts i and c represent, respectively, the ith phase and the composite consisting of N phases,

$$\sum_{i=1}^{N} V_i = 1 \qquad (2.2)$$

2.1.2. Characteristics of GMR

Effects of microstructures are expressed by a scaling, fractal parameter J, which is mainly controlled by the shape, size distribution, and distribution (continuity and

connectivity) of the phases (Ji, 2004a and b). According to Ji (2004), $M_c(J)$ has the following characteristics:

(a) $M_c(J)$ is a continuous, monotonous increasing function for all J values in the ranges ($-\infty \leq J \leq \infty$). This monotonicity stands with respect to either the volume fractions or the physical properties.

(b) For $J<1$, $J=1$ and $J>1$, $M_c(J)$ as a function of the individual grades of membership M_i is strongly concave, linear, and strongly convex, respectively.

(c) For a binary system that consists of a strong phase (s) and a weak phase (w), $J<0$ for the weak-phase supported structure while $J>0$ for the strong-phase supported structure (Ji, 2004a and b). The GMR fulfills the following boundary conditions: for $V_s=0$ (pure weak phase aggregate), the effective properties are equivalent to the properties of the weak phase for all values of J. Similarly, for $V_s=1$ (pure strong phase aggregate), the effective properties are equivalent to the properties of the strong phase for all values of J. In the circumstance that $M_s=M_w$ (two phases have an equivalent property), then $M_c=M_s=M_w$ for all values of J and all values of V_s.

(d) The case $J=1$ yields the arithmetic mean or Voigt average (which assumes constant strain). The case $J=-1$ yields the harmonic mean or Reuss average (which assumes constant stress). For isotropic composites, the Voigt and Reuss averages are generally regarded as the upper and lower bounds for effective elastic properties (Hill, 1965). For a composite consisting of rigid particles in a steady-state flowing matrix, however, its effective creep strength may be lower than the Reuss bound as long as the stress exponent of the matrix is sufficiently large, say, ≥ 4 (Ji et al., in press). The GMR with $J \rightarrow 0$ yields the geometrical mean. The latter becomes physically meaningless when one of the constituent phases has a null property. In this special case, the overall property of the composite acquired from the geometrical mean will always vanish regardless of the volume fraction of the constituent that has a null property.

the volume fraction of the constituent that has a null property.

2.1.3. Applications of GMR

Ji et al. (2004) found that the GMR with J=0.5 and J=-0.5 provides good agreement with the experimental data of Young's modulus for the two-phase composites in which inclusions are shaped like spheres isolated in a continuous, stronger and weaker host mediums, respectively. For most composite materials in which the inclusions are of somewhat arbitrary geometry, the GMR with J=-0.25 and J=0.25 does well at predicting the measured values of Young's modulus for those with weak-phase continuous ($V_s \leq 0.5$) and strong-phase continuous ($V_s \geq 0.7$) structures, respectively. In the intermediate range ($0.5 \leq V_s \leq 0.7$), J was found to vary progressively from -0.5 to 0.5 or from -0.25 to 0.25 due to the transition in microstructure.

Recently, Ji (2004) showed that various celebrated expressions such as Einstein's equation for ideal, dilute suspensions (Einstein, 1906) and Roscoe's formula for general solid-liquid suspensions (Roscoe, 1952) can be derived as special cases from the GMR using the microstructural parameter J=-0.4. It has been demonstrated that the GMR works well for describing various mechanical properties (e.g., elastic moduli, hardness, yield, and flow strengths for wide ranges of multiphase systems from natural rocks to industrial ceramics and alloys).

2.2. Analysis of GMR

For a two-phase composite, Eq. (2.1) can be simplified:

$$M_c^{\ J} = (1 - V_w) M_s^{\ J} + V_w M_w^{\ J} \tag{2.3}$$

Porous materials can be considered as a special class of two-phase composites in which null strength pores are dispersed within a solid framework. Then setting the mechanical property of the weak phase equals to zero (i.e., M_w=0) and taking V_w as the volume fraction porosity (p) allow an estimation of the effect of porosity on the property. Eq. (2.3) can be written as

$$\frac{M_c}{M_s} = (1 - p)^{1/J} = V_s^{\ 1/J} = \left(\frac{\rho_c}{\rho_s} \right)^{1/J} \tag{2.4}$$

where J is the microstructural parameter that depends on the geometrical shape, spatial arrangement, orientation and size distribution of pores, and in turn on the materials and the fabrication method (i.e., cold pressing, sintering, or hot isostatic pressing), ρ_c and ρ_s are the densities of the porous and nonporous materials, respectively. ρ_c/ρ_s is the relative density that equals the volume fraction mass. On the plots of $\log(M_c/M_s)$ versus $\log(1\text{-}p)$ or $\log(\rho_c/\rho_s)$, $1/J$ is the slope of the property dependence over the linear range. The value of J should lie in the range from 0 to 1, giving a wide range of properties at a given relative density or porosity. The variation of J with microstructure yields a large possibility to optimize the mechanical properties of porous solids. Further, porosity has a greater effect on the mechanical properties at smaller values of J.

J=1 for porous materials with long cylindrical or hexagonal pores aligned parallel to the stress direction,

$$\frac{M_c}{M_s} = 1 - p = \frac{\rho_c}{\rho_s} \tag{2.5}$$

Eq. (2.5) yields a linear relationship between M_c/M_s and p, and good agreement with experimental results of lotus-type porous metals with the elongated pores parallel to the loading direction (Hyun et al., 2001; Ichitusubo et al., 2002), see Figure 2.1. J=0 represents an extreme case where the effective property of a porous material will vanish, regardless of porosity.

Generally, intergranular, continuous, channel pores or cavities cause a lower J value than intragranular, isolated and rounded pores. The open pores exhibit a lower J value and thus more pronounced effects on the effective mechanical properties than the closed pores. Thus, the complex dependence of J on microstructure is a crucial subject for study in order to better predict and optimize the mechanical properties of porous solids.

Eq. (2.4) can be expanded to a power series:

$$\frac{M_c}{M_s} = 1 + \left(-\frac{1}{J}p\right) + \frac{\frac{1}{J}\left(\frac{1}{J}-1\right)}{2}p^2 + \frac{\left(-\frac{1}{J}\right)\left(\frac{1}{J}-1\right)\left(\frac{1}{J}-2\right)}{6}p^3 + \cdots\cdots \tag{2.6}$$

For low values of porosity (p <<1), Eq. (2.6) can be reasonably approximated by

$$\frac{M_c}{M_s} = 1 - \frac{1}{J}p \tag{2.7}$$

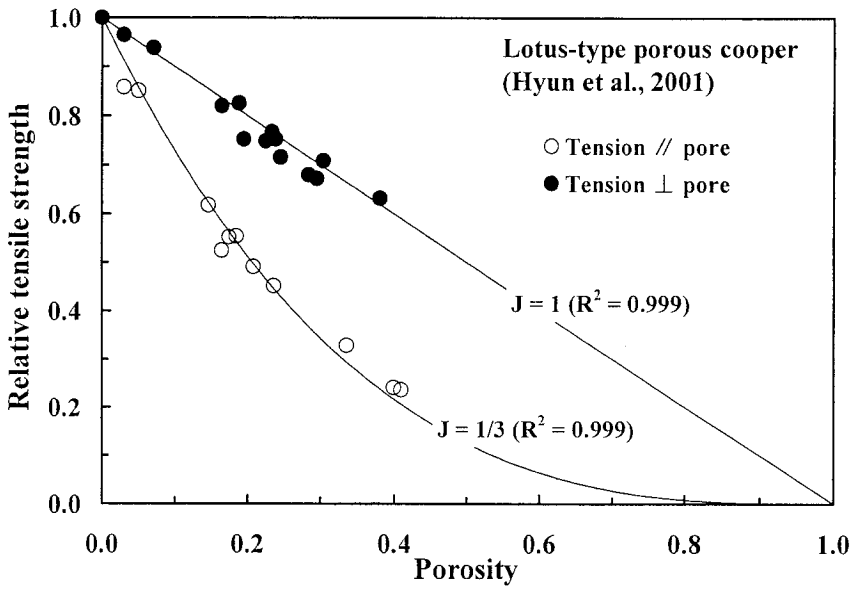

Figure 2.1 Relative tensile strengths of lotus-type porous cooper as a function of porosity. Theoretical curves labeled according to J values.

Eq. (2.7) indicates a linear relation between M_c/M_s and p at low porosities (p <0.10-0.15).

The pore shape, which is one of the most important factors to affect the J value, can be characterized by the shape factor (S) that is defined below:

$$S=4\pi A/L^2 \qquad (2.8)$$

where A is the pore area and L is the pore perimeter in a random thin section. Both A and L can be determined using quantitative image analysis. S decreases in magnitude as the pore outline becomes more irregular. For example, S=1 for a perfect circle, S=0.785 for a square, S=0.604 for equilateral triangle, and S approaches zero if the pore shape

becomes a line (Russ, 1986). It is found that spherical pores generally occur at low porosities. As the porosity increases, the shape factor decreases and the pore geometry becomes increasingly more complex. When the porosity is higher than a critical value (p_{c1}), the pores become increasingly more open (Nielsen, 1982). Thus, p_{c1} is the critical porosity at which a transition occurs from isolated and closed pores to open and interconnected pores. Moreover, large pores are generally more irregular than small pores, indicating that the large pores may form from the agglomeration of small pores. As a result, the S value decreases (Beiss et al., 2001) and so does the J value with increasing pore size. Conversely, a trend of decreasing S with decreasing pore size may result if small irregular pores were produced by fragmentation of large smooth ones. Thus, the J value may reflect the formation processes of the materials.

Furthermore, the mechanical properties of a nonporous material can be estimated from its porous counterpart according to the following equation:

$$M_s = \left[\frac{M_c^{\,J}}{1-\phi}\right]^{1/J} \tag{2.9}$$

An analytical formula such as Eq. (2.9) is much more advantageous than complicated and tedious computational codes if one desires to invert the mechanical property of a porous material to that of its non-porous counterpart if the porosity and pore geometry are known.

2.3 Comparison of GMR with other expressions

In this section, we will illustrate that the GMR is a good descriptive model to fit the experimental data for the elastic and plastic mechanical properties of porous materials (i.e., $M_s/M_w \rightarrow 0$).

Because it is obviously prohibitive to determine experimentally the effective properties of each porous material of interest, numerous empirical and theoretical relations have been proposed to describe the dependence of mechanical property of materials to their porosities. The empirical relations attempt to best-fit experimental data, but the physical meaning of the relations is unclear. However, the theoretical models, in spite of using the first physical principles, are based on some idealized microstructures (e.g., uniform spherical, cylindrical or cubic pores are arranged in a cubic array (Eudier, 1962; Paul, 1960; Gibson and Ashby, 1988; Rice, 1998)), and the derived correlations between the effective properties and porosity often cannot be extended to real materials with irregular shapes, non-uniform size and random distribution of pores.

One of the most popular expressions is the following:

$$\frac{M_c}{M_s} = (1-p)^m \qquad (2.10)$$

where m is an adjustable parameter. In Eq. (2.10), M represents the Young's modulus (E), shear modulus (G), bulk modulus (K), yield strength (σ_y), rupture strength (σ_r), or flow strength (σ_f). Eq. (2.10) was first proposed by Balshin (1949) as an empirical equation. Based on the assumption that a porous material consists of a three-dimensional (3D) intertwined, continuous network of material chains and open-pore channels, Wong et al. (1984) and Wagh et al. (1991) derived Eq. (2.10) as a theoretical formula for the porosity dependence of the Young's modulus. These authors named the expression as the connected-grain or open pore model.

The comparison of Eq. (2.10) with Eq. (2.4) yields m=1/J. In the elastic field, the exponent m has been related to the stress concentrations that develop around pores

(Haynes, 1971; Griffiths et al., 1979), and named as the elastic stress concentration factor of the pores (Ichitsubo, 2002; Phani, 1986; Boccacini et al., 1995; Blanks, 1998). Based on 3D elasticity theory for the stress concentration around spheroidal pores (Z is the axis of revolution and X is the axis perpendicular to Z) in a material under uniaxial stress, Boccaccini et al. (1995) obtained the following results. For spherical pores (Z/X=1), m=2 and thus J=0.5. For infinitely long cylindrical pores (Z/X$\rightarrow\infty$) oriented perpendicular to the stress direction, m=3 and thus J=1/3 (Figure 2.1). For lotus-type porous materials with long cylindrical or hexagonal pores (Z/X$\rightarrow\infty$) oriented parallel to the stress direction, there is no stress concentration effect (Rice, 1997) and $m\rightarrow 1$ or $J\rightarrow 1$ (Figure 2.1).

The porosity dependence of physical properties of porous materials can be evaluated using an assumption that the relative property of interest (M_c/M_s) is equal to the ratio of the minimum solid area (MSA) to the cell area normal to the reference stress (Rice, 1998). The MSA can be easily calculated for idealized structures, that is, regular stacking of uniform (spherical, spheroidal, cylindrical or cubic) pores in a continuous solid medium (Eudier, 1962; Paul, 1960). The variations of the MSA with porosity have been studied for various ordered arrays of pores. It is generally found that the MSA can be related to the porosity for relatively low volume fraction of porosity ($p\leq\sim 0.4p_c$, where p_c is the critical porosity that corresponds to the percolation limit of the solid phase) by an exponential function (Rice, 1998; Knudsen, 1959; Rice, 1977):

$$\frac{A}{A_0} = \exp(-bp) \qquad (2.11)$$

where A and A_0 are, respectively, the solid areas of porous and porosity-free materials, normal to the reference direction; and b is a constant that depends on the array of pores in the material. In other words, the value of $\ln(A/A_0)$ decreases linearly with the porosity with b equal to the slope.

As the relative value of M_c/M_s is directly proportional to that of A/A_0 (Rice, 1998), thus:

$$\frac{M_c}{M_s} = \exp(-bp) \qquad (2.12)$$

Eq. (2.12) was proposed first by Duckworth (Duckworth, 1951) as an empirical equation and since then it has been widely used to predict the effective mechanical properties of porous materials with reasonable accuracy (Rice, 1998; Knudsen, 1959; Rice, 1977; Spriggs, 1961). According to Ramakrishan and Arunachalam (Ramakrishnan et al., 1993), Eq. (2.12) can be obtained using the differential methods (Mclaughlin, 1977; Norris, 1985; Zimmerman, 1991) under certain approximations.

Unlike Eq. (2.4), Eq. (2.12) displays an evident disadvantage: the boundary condition that M_c should be equal to zero when p is equal to 1 is not satisfied (Hasselman, 1962). Actually Eq. (2.12) breaks down when $p \rightarrow p_c$. Consequently, Eq. (2.12) is not valid over the full range of porosity from 0 to 1 and can be used for only low values of porosity (i.e., $p \leq 0.30$).

Eq. (2.12) can be expanded to a power series:

$$\frac{M_c}{M_s} = 1 + (-bp) + \frac{(-bp)^2}{2} + \frac{(-bp)^3}{6} + \cdots\cdots \qquad (2.13)$$

For low values of porosity (i.e., $p << 1$), Eq. (2.13) can be reasonably approximated by the first term of the above series expansion.

$$\frac{M_c}{M_s} = 1 - bp \qquad (2.14)$$

Eq. (2.14) yields the same formula as that proposed by Hashin (1968) and Rossi (1968).

Comparison between Eq. (2.7) and Eq. (2.14) gives

$$J = \frac{1}{b} \qquad (2.15)$$

J is the inverse of b. For many porous materials, the b values have already been determined and can be converted to the J values (Table 2.1).

For many porous polycrystalline materials, the b values have been determined for each property and can be converted to the J values (Figure 2.2). Therefore, the exponential expression as described by Eq. (2.12) can be derived directly from the GMR for the porous materials with relatively low values of porosity (p <<1 where there are most data).

Considering the linear-elastic edge deflection of open-cell foams, Gibson and Ashby (1988) pursued a simple relation for the Young's modulus of the cellular solids:

$$\frac{E_c}{E_s} = C\left(\frac{\rho_c}{\rho_s}\right)^n = C(1-p)^n \qquad (2.16)$$

where C and n are constants that depend on the microstructure of the foam. Setting ρ_c equal to ρ_s or p=0 in Eq. (2.16) does not yield the boundary condition that E_c is equal to

E_s if C≠1. To satisfy this boundary condition will require C=1 and in turn Eq. (2.16) becomes identical to our Eq. (2.4) with J=1/n.

Table 2.1 The J values obtained by fitting the GMR with experimental results for Young's modulus of various materials.

Porous material	Source of data	Porosity range	E_0 (GPa)	J
Oxides				
Al_2O_3 (fibers)	Blakelock et al., 1970		373	0.256
Al_2O_3	Neuber & Wimmer, 1968	0.03-0.18	340	0.313
Al_2O_3	Coble & Kingery, 1956	0.15-0.55	390	0.357
Al_2O_3	De Portu & Vincezini, 1979	0.08-0.31	420	0.244
Al_2O_3	Wang, 1984	0.05-0.43	400	0.25
Al_2O_3	Binns & Popper, 1966	0-0.100	280	0.345
Al_2O_3	Wu & Rice, 1985	0.02-0.40	400	0.385
β-Al_2O_3	Barnaby & Taylor, 1972	0-0.41		0.243
β-Al_2O_3	Evans et al., 1984	0.01-0.38	215	0.2
Al_2O_3	Knudson, 1962	0-0.30	411	0.284
Al_2O_3	Sprggs et al., 1961	0-0.40	411	0.263
Al_2O_3	Knudsen, 1962			0.253
Al_2O_3	Spriggs, 1962	0-0.40		0.287
Al_2O_3	Spriggs & Vasilos, 1961			0.229
Al_2O_3	Spriggs, 1961			0.253
B_6O	Rice, 1977		459	0.217
B_6O	Petrak et al., 1974	0-0.08	475	0.25
BeO	Chandler et al., 1963	0.02-0.17	410	0.435
BeO	O'Neill & Livey, 1965	0-0.07	400	0.27
CeO_2	Argoitia et al., 1987	0.03-0.09	205	0.357
MgO	Spriggs et al., 1962	0-0.40	317	0.241
MgO	Janowski & Rossi, 1968	0-0.115	305	0.244
MgO	Biddulph, 1964	0.05-0.30	270	0.27
CoO	Petrak et al., 1975	0.09-0.20	230	0.222
Nb_2O_5	Manning et al., 1969	0-0.18	150	0.196
SiO_2	Gannon et al., 1965		72	0.152
SiO_2	Tomilov, 1977	0.01-0.19	70	0.185
SiO_2	Harris & Welch, 1973	0.01-0.18	70	0.313
Sm_2O_3	Hunter et al., 1974	0.02-0.37	145	0.286
Sm_2O_3	Dole et al., 1977	0.02-0.24	145	0.179
Y_2O_3	Marlowe & Wilder, 1965	0.05-0.37	180	0.227

Table 2.1 (continued)

Porous material	Source of data	Porosity range	E_0 (GPa)	J
Y_2O_3	Manning et al., 1969	0.04-0.22	180	0.357
Er_2O_3	Manning et al., 1969	0.05-0.21	180	0.345
Dy_2O_3	Manning et al., 1969	0.03-0.19	170	0.357
Gd_2O_3	Haglund & Hunter, 1973	0.025-0.367	310	0.244
Ho_2O_3	Manning et al., 1969	0-0.18	170	0.385
Lu_2O_3	Hunter & Graddy, 1976	0.03-0.33	193	0.238
H_2O (ice)	Tabata, 1967		14	0.213
ThO_2	Petersen & Curtis, 1970		239	0.294
ThO_2	Spinner et al., 1963	0.07-0.40	260	0.25
ThO_2	Curtis & Johnson, 1957	0.05-0.41	280	0.294
UO_2	Boocock et al., 1972	0-0.28	225	0.303
UO_2	Panckkal & Ghosh, 1984	0.05-0.10	270	0.244
TiO_2	Chung & Bussem, 1968		282	0.37
ZrO_2	Smith & Crandall, 1964		249	0.238
Metals				
Fe	Panakkal et al., 1990	0.03-0.127	223	0.265
Borides				
TaB_2	Claussen, 1969		445	0.2
TiB_2	Mandorf & Hartwig, 1963	0.03-0.20	546	0.27
ZrB_2	Clougherty et al., 1968		524	0.323
Carbides				
B_4C	Liebling, 1967	0-0.09	480	0.175
B_4C	Champagne & Anger, 1979	0.08-0.30	280	0.182
B_4C	Beauvy, 1982	0-0.30	445	0.2
B_4C	Wu & Rice, 1985	0-0.15	500	0.25
B_4C	Schwetz et al., 1986	0-0.25	435	0.294
NbC	Speck & Miccioli, 1968		520	0.294
SiC	Croxet et al., ?	0.02-0.27	440	0.204
SiC	Prochazka et al. 1974	0.03-0.28	480	0.323
SiC	Reynaud et al., 2004	0-0.42	407	0.373
SiC	Coppola & Bradt, 1972	0.02-0.16		0.263

Table 2.1 (continued)

C	Source of data	Porosity range	E_0 (GPa)	J
SiC	Carnahan, 1968	0-0.15	448	0.239
ZrC	Jun & Shaffer, 1971		445	0.313
Nitrides				
Si_3N_4	Datta et al., 1989	0-0.38	300	0.303
Si_3N_4	Yeheskel & Gefen, 1985	0-0.36	310	0.2
Si_3N_4	Bubnov et al., 1986	0-0.40	300	0.25
Si_3N_4	DePorto & Vincenzini, 1980	0-0.35	290	0.175
Si_3N_4	Larson et al., 1977	0-0.27	315	0.323
Si_3N_4	Hasselman & Fulrath, 1964;	0-0.20		0.388
TaN	Desmaison-Brut et al., 1991	0-0.15	515	0.217
TiN	Desmaison-Brut et al., 1991	0-0.22	475	0.333
ZrN	Desmaison-Brut et al., 1991	0.02-0.08	390	0.303
Si_2N_2O	Boch & Gandus, 1979	0-0.27	220	0.27
Carbon & graphite				
C (fibers)	Ezekiel, 1970		11.78	0.152
C (fibers)	Butler, 1973		11.85	0.111
Graphite	Cost et al., 1968	0.13-0.32	255	0.286
Graphite	Wagner et al., 1972		32.38	0.196
Alloys				
Ti-24Al-11Nb	Matikas et al., 1997	0-0.30	94.9	0.227
Other materials				
Gypsum (I)	Soroka & Sereda, 1968	0.45-0.70	44.1	0.34
Gypsum (II)	Soroka & Sereda, 1968	0-0.45	51.3	0.22
Gypsum (IV)	Soroka & Sereda, 1968	0-0.3	51.2	0.38
Gypsum (V)	Soroka & Sereda, 1968	0-0.3	48.4	0.12
Gypsum (I + IV)	Soroka & Sereda, 1968	0-0.70	54.3	0.33
Clay	Heindl & Pendergast, 1927		6.89	0.238
Mixtures				
CoO-MgO	Petrak et al., 1975	0.06-0.16	260	0.227
$CoAl_2O_4$	Petrak et al., 1975	0.03-0.14	225	0.185
Li_4SiO_4	Chu et al., 1989	0.07-0.32	140	0.256
$MgAl_2O_4$	Schreiber, 1968		280	0.238

Table 2.1 (continued)

Porous material	Source of data	Porosity range	E_0 (GPa)	J
$MgAl_2O_4$	Schreiber, 1968		112	0.244
$MgAl_2O_4$	Porter et al., 1977	0-0.32	299	0.27
$Si_3N_4 + MgO$	Portu & Vincenzini, 1981	0-0.45		0.182
$Si_3N_4 + CeO_2$	Portu & Vincenzini, 1981	0-0.38		0.238
$Si_3N_4 + Y_2O_3 +$	Portu & Vincenzini, 1981	0-0.12		0.262
Al_2O_3+MgO	Kathrina et al., 1991	0-0.33	67	0.146
SiC + 10 wt.% YAG	Reynaud & Thevenot, 2000	0-0.20	445	0.287
Ferrite	Chen & Weisz, 1972		89.6	0.244
Mullite	Penty et al., 1972	0-0.13	230	0.285
$YBa_2Cu_3O_7$	McAlford et al., 1988	0-0.24	180	0.27

Table 2.2. The J values obtained by fitting the GMR with experimental results using the least squares regression analysis for shear moduli (G) of polycrystalline aggregates.

Porous material	Source of data	Porosity range	G_0 (GPa)	J
Al_2O_3	Knudsen, 1961; Neuber & Wimmer, 1971		165	0.303
Al_2O_3	Coble & Kingery, 1956	0.15-0.55	164	0.357
B_6O	Rice, 1977		198	0.222
B_6O	Petrak et al., 1974		203	0.25
BeO	Rice, 1977		161	0.333
MgO	Sprggs et al., 1962	0-0.40	132	0.204
Sm_2O_3	Hunter et al., 1974	0.02-0.37	55	0.37
Sm_2O_3	Dole et al., 1977	0.02-0.24	55	0.204
Y_2O_3	Manning et al., 1969	0.04-0.22	69	0.37
Er_2O_3	Manning et al., 1969	0.05-0.21	70	0.345
Dy_2O_3	Manning et al., 1969	0.03-0.19	64	0.385
Ho_2O_3	Manning et al., 1969	0-0.18	67	0.385
Lu_2O_3	Hunter & Graddy, 1976	0.03-0.33	75	0.244
ThO_2	Petersen & Curtis, 1970		110	0.25
ThO_2	Spinner et al., 1963	0.07-0.40	100	0.167
UO_2	Boocock et al., 1972	0-0.28	85	0.286
Fe	Panakkal et al., 1990	0.03-0.127	86	0.286
B_4C	Liebling, 1967	0-0.09	204	0.175
B_4C	Schwetz et al., 1986	0-0.25	190	0.263
SiC	Carnahan, 1968	0-0.15	192	0.233
Si_3N_4	Fate, 1974	0-0.27	125	0.313
TaN	Desmaison-Brut et al., 1991	0-0.15	205	0.286
TiN	Desmaison-Brut et al., 1991	0-0.22	195	0.357
ZrN	Desmaison-Brut et al., 1991	0.02-0.08	155	0.27
Si_2N_2O	Boch & Gandus, 1979	0-0.27	90	0.286
Graphite	Cost et al., 1968	0.13-0.32	97	0.303
Graphite	Wagner et al., 1972		15.16	0.227
Ti-24Al-11Nb	Matikas et al., 1997	0-0.30	35	0.248
Li_4SiO_4	Chu et al., 1989	0.07-0.32	55	0.263
$MgAl_2O_4$	Porter et al., 1977	0-0.32	118.5	0.28
SiC + 10 wt.% YAG	Reynaud & Thevenot, 2000	0-0.20	189	0.29

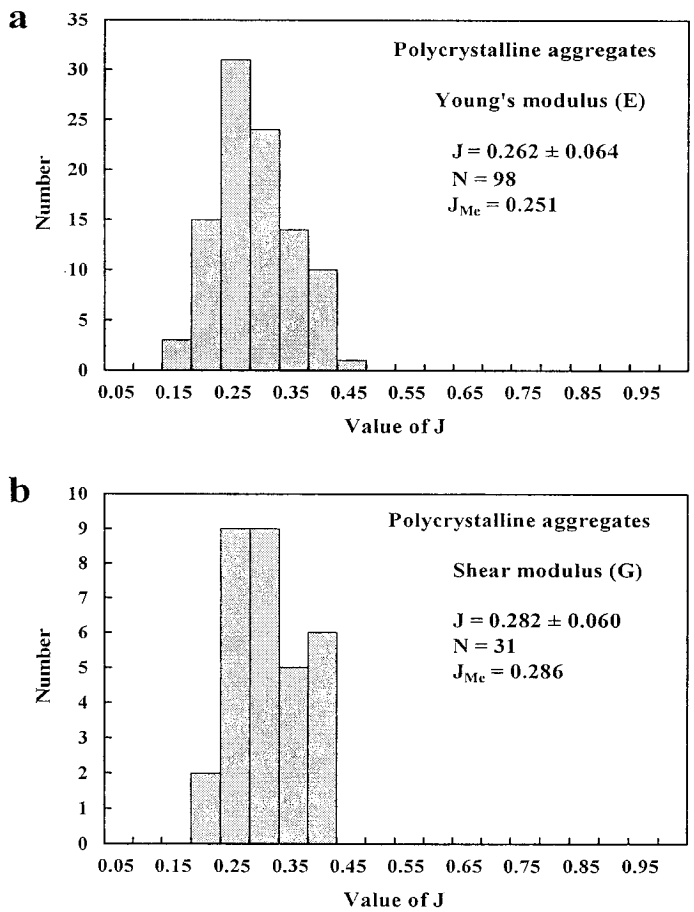

Figure 2.2 Histograms of J values for the Young's modulus (a) and shear modulus (b) of polycrystalline aggregates. Data mainly from R.W. Rice (1998). N, the number of measurements; J_{Me}, the median (the fiftieth percentile in the distribution).

Fitting the experimental data (Lederman, 1971; Gent, 1959; Gibson, 1982) with Eq. (2.16), Gibson and Ashby (1988) obtained n=2, which corresponds J=0.5 in Eq. (2.4). In the case of porous materials with a honeycomb structure, Gibson and Ashby (1988) show that n=1 (i.e., J=1) and n=3 (J=1/3) for the directions parallel to and perpendicular to the direction of pores, respectively (Figure 2.1).

Based on an assumption that the relative property of interest (M_c/M_s) equals the ratio of the minimum solid area (MSA) to the cell area normal to the reference stress, and using an ideal microstructure that uniform spherical pores are arranged in a simple cubic array, Eudier (1962) obtained

$$\frac{M_c}{M_s} = 1 - \pi\left(\frac{3}{4\pi}\right)^{2/3} p^{2/3} = 1 - 1.21p^{2/3} \qquad (2.17)$$

In Eudier's model, the critical value of p for the cubic packing geometry is $\pi/6$ or 0.524, over which the pores should overlap each other. In other words, a transition from isolated and closed to open and interconnected porous structures occurs when $p \geq 0.524$. Moreover, M_c/M_s will reach zero once $p = 4/\left(3\sqrt{\pi}\right)$ or 0.752. For $p > P_c = 0.752$, Eq. (2.17) becomes no longer valid. At $p \leq 0.30$, the Eudier's model can be approximated by the GMR with J=0.410 (Figure 2.3).

Further, Ramakrishnan and Arunachalam (1990) derived the following equation for an isolated spherical pore geometry:

$$\frac{M_c}{M_s} = \frac{\left(1 - p^2\right)}{1 + \beta p} \qquad (2.18)$$

where β is a parameter that is a function of zero-porosity Poisson's ratio (υ_0) of the solid matrix.

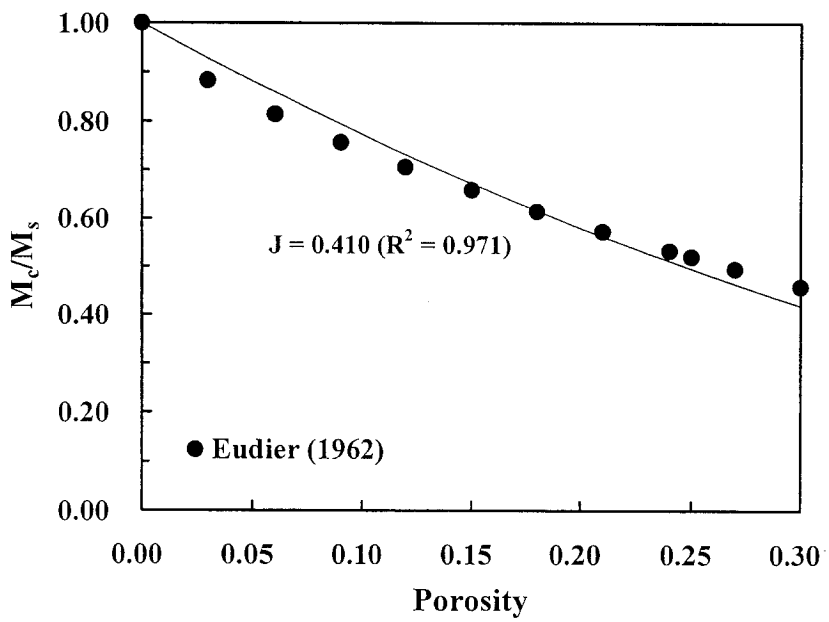

Figure 2.3 Comparison of the GMR with the theoretical models of Eudier (1962).

$$\beta_K = \frac{1+\upsilon_0}{2(1-2\upsilon_0)} \tag{2.19}$$

$$\beta_G = \frac{11-19\upsilon_0}{4(1+\upsilon_0)} \tag{2.20}$$

$$\beta_E = 2 - 3\upsilon_0 \qquad (2.21)$$

for the bulk (K), shear (G) and Young's (E) moduli, respectively. $\beta_K = \beta_G = \beta_E = 1.25$ when $\upsilon_0 = 0.25$. Eq. (2.18) can be represented by the GMR. For example, the case of $\beta = 1.25$ is approximately equivalent to $J = 0.509$ (Figure 2.4).

For solids containing cubic pores,

$$\frac{M_c}{M_s} = 1 - kp^{2/3} \qquad (2.22)$$

where $k = 1$, $\sqrt{2}$ and $\sqrt{3}$ for cubic pores with their <100>, <110> and <111> directions parallel to the reference direction, respectively (Rice, 1998; Ishai and Cohen, 1967). Eq. (2.22) with $k = 1$, $\sqrt{2}$ and $\sqrt{3}$ can be approximated, respectively, by the GMR with $J = 0.507$, 0.321 and 0.237 at $p \leq 0.26$ (Figure 2.5). Clearly, the J value decreases progressively as the cubic pores are oriented with their <100>, <110> and <111) directions parallel to the reference direction.

It is necessary to point out that the theoretical models summarized above, which were based on specific structures, cannot be extended to more general materials with irregular shapes, varied size and random distribution of the pores.

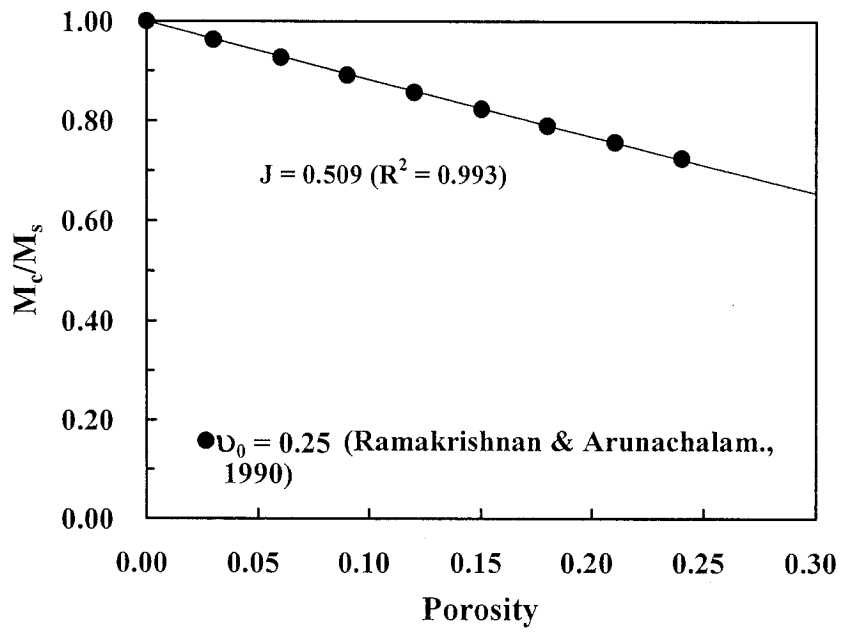

Figure 2.4 Comparison of the GMR with the theoretical models of Ramakrishnan and Arunachalam (1990).

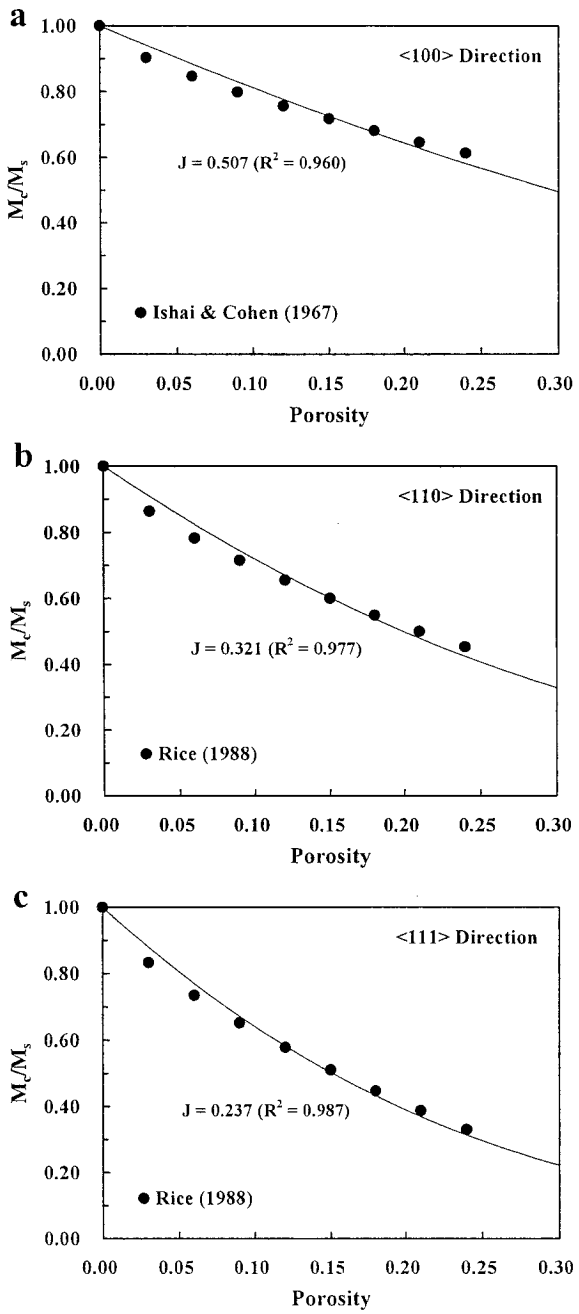

Figure 2.5 Relative mechanical properties of solids containing cubic pores with their <100> (a), <110> (b) and <111> (c) directions parallel to the loading direction.

The microstructural evolution of a material with increasing porosity is a 3D connectivity problem. According to the percolation theory (Stauffer et al., 1992), there may exist two critical porosity levels. When the porosity reaches the first critical value (p_{c1}), a microstructural transition occurs from fully isolated and closed pores with nearly spherical or ellipsoidal shapes to open and interconnected with complex shapes. Finally, the effective strength or elastic modulus vanishes when the porosity reaches the second critical value (p_c). For polycrystalline materials composed of identical spherical particles arranged in cubic, orthorhombic and rhombohedral arrays, Knudsen (Knudsen, 1959) obtained the theoretical p_c values of 0.476, 0.397 and 0.26, respectively. For powder materials, the p_c value seems to be the apparent porosity of the powder before densification by sintering or hot pressing (Kovacik, 1999). Therefore, three regimes can be identified: (1) At low porosity levels ($p<p_{c1}$), pores are fully isolated and closed with nearly spherical or ellipsoidal shapes; (2) At intermediate porosity levels ($p_{c1}\leq p<p_c$), interconnected pores with complex shapes are present; (3) The stress-supporting solid framework fails when $p\geq p_c$.

One important consequence of the microstructural transition at p_{c1} is that the mechanical properties of porous materials in regime 2 ($p_{c1}\leq p<p_c$) cannot be represented by Eq. (2.4); if this is attempted then there will be an apparent decrease in J with increasing p. Thus, p in Eq. (2.4) for the intermediate regime may be replaced reasonably by the effective porosity (p/p_c) due to the interconnection of pores.

$$\frac{M_c}{M_s}=\left(1-\frac{p}{p_c}\right)^{1/J} \qquad (2.23)$$

with $p\leq p_c$ and $p_c\leq 1$. Eq. (2.23) yields the same formula proposed by Phani (1986) as an empirical equation for the Young's modulus-porosity relation in gypsum systems.

Chapter 3. Comparison with experiments

In this chapter, the results calculated by GMR will be compared with experimental data. Figures 3.1– 3.7 show a set of examples for the comparison between the experimentally measured relative Young's modulus (E_c/E_s) and the theoretical values calculated by GMR. The goodness of the consistence between theoretical and experimental data is evaluated according to a parameter so-called variance (R^2). The more R^2 approaches to 1, the best the consistence is between the theory and experiment. The J-value is calculated from the experimental data using the least-square method, which is a classical statistical approach. As shown in Fig. 3.1, the experimental data for porous Al_2O_3 polycrystalline aggregates with porosities ≤30% (Knudson, 1962) can be fitted with Eq. (2.23) (J=0.284 and p_c=1). As illustrated in Fig. 3.2, Eq. (2.23) with J=0.263 and p_c=1 yields a good fit to experimental data for porous Al_2O_3 with p≤40% (Spriggs, 1961). Experimental data for porous MgO aggregates with p≤40% (Spriggs, 1962) are in good agreement with Eq. (2.23) using J=0.241 and p_c=1 (Fig. 3.3). Eq. (2.23) with J=0.370 and p_c=1 works very well for fitting the experimental data for polycrystalline SiC aggregates with p≤42% (Reynaud et al., 2005, Fig. 3.4). Porter et al. (1977) studied the elasticity of polycrystalline spinel ($MgAl_2O_4$) aggregates prepared by hot pressing. Their data on the porosity-dependence of Young's and shear moduli are consistent with the GMR with J=0.270 (Fig. 3.5) and J=0.280 (Fig. 3.6), respectively. For phosphate-bonded, alumina filled, magnesia ceramics dominated by shaped-cornered holes and flat elliptical cavities (Kathrina et al., 1991), however, the experimental data (Fig. 3.7) are well fitted by the GMR with J=0.146, p_c=1.

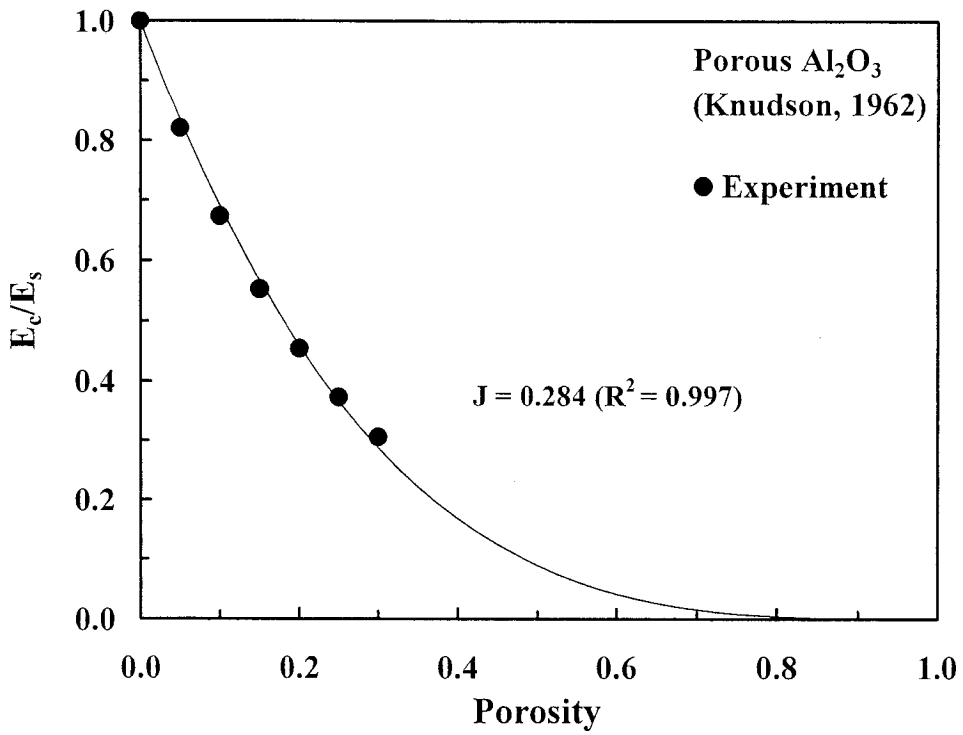

Figure 3.1 Comparison of the theoretical values calculated from the GMR with experimental data on relative Young's modulus of porous material Al_2O_3 (Knudson, 1962).

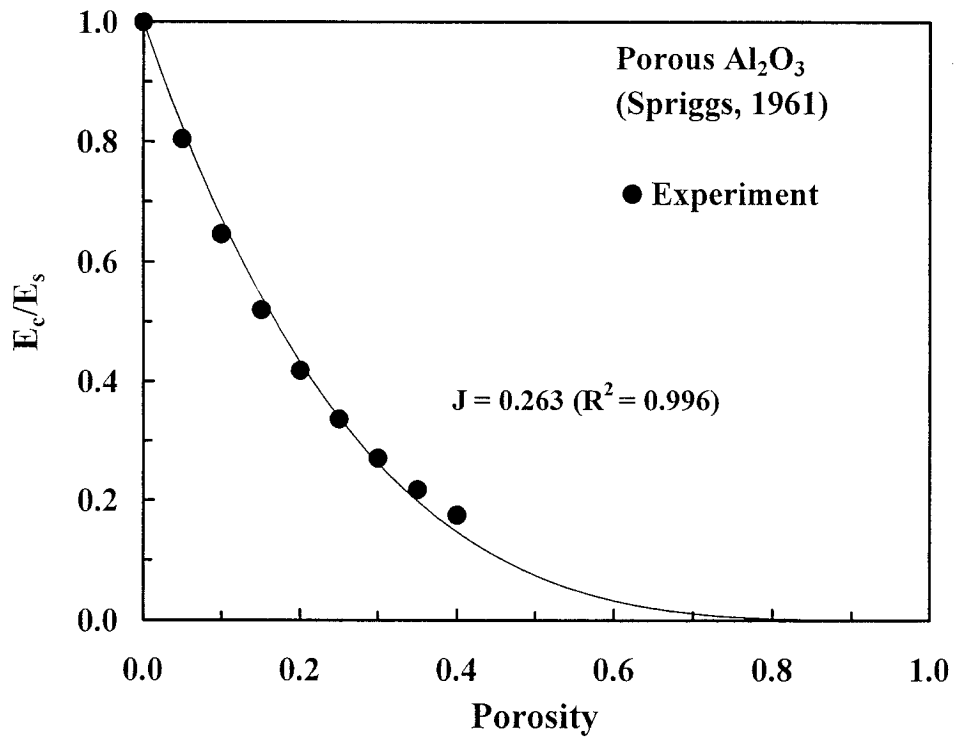

Figure 3.2 Comparison of the theoretical values calculated from the GMR with experimental data on relative Young's modulus of porous material Al_2O_3 (Spriggs, 1961).

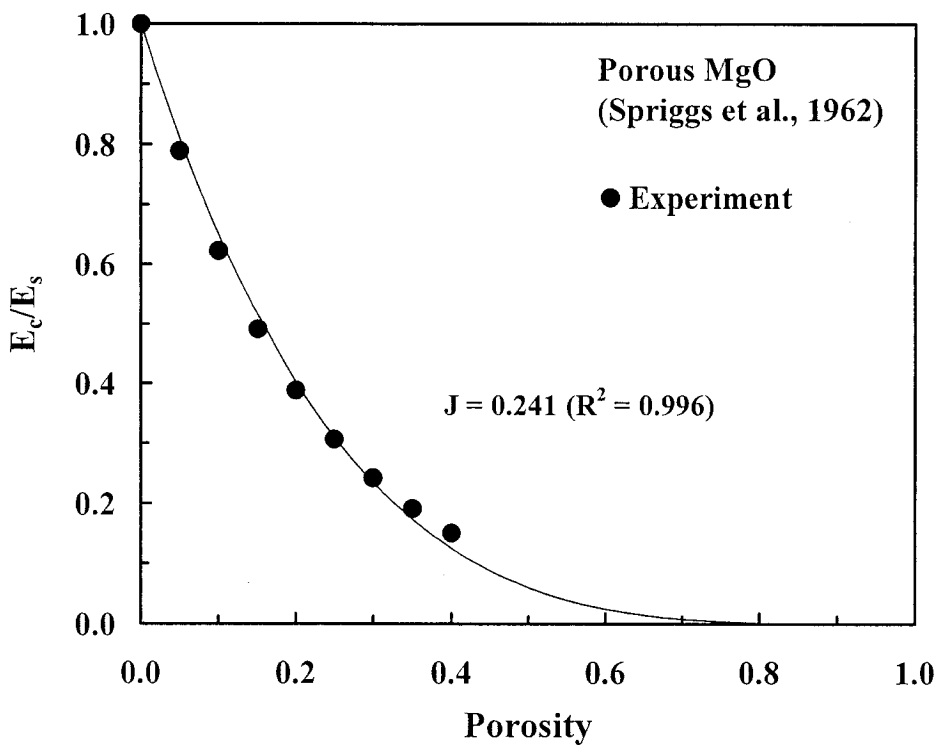

Figure 3.3 Comparison of the theoretical values calculated from the GMR with experimental data on relative Young's modulus of porous material MgO (Spriggs, 1962).

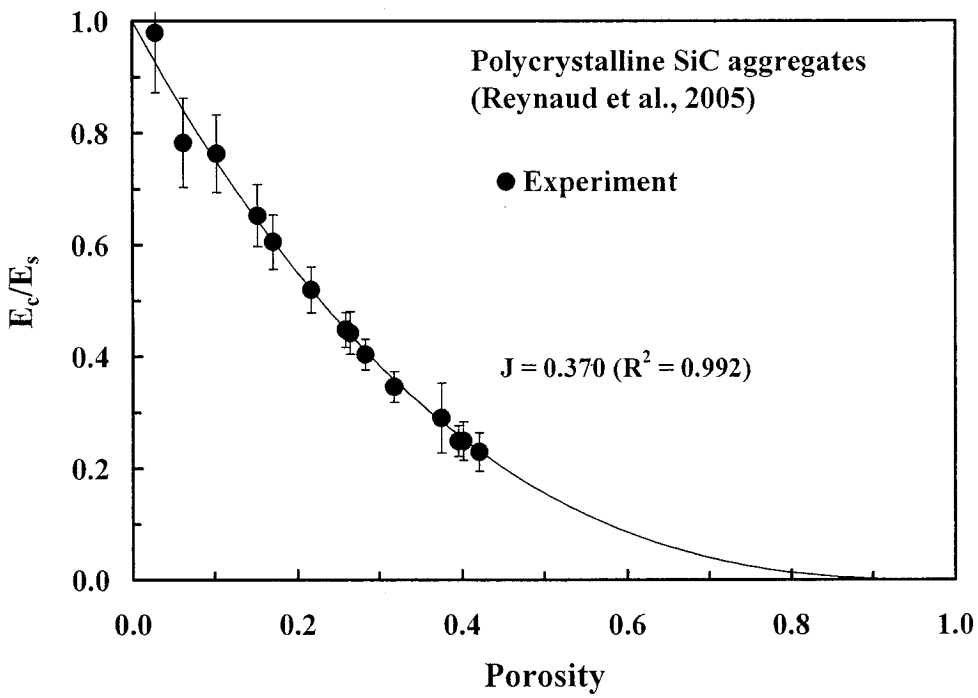

Figure 3.4 Comparison of the theoretical values calculated from the GMR with experimental data on relative Young's modulus of porous material SiC (Reynaud et al., 2005).

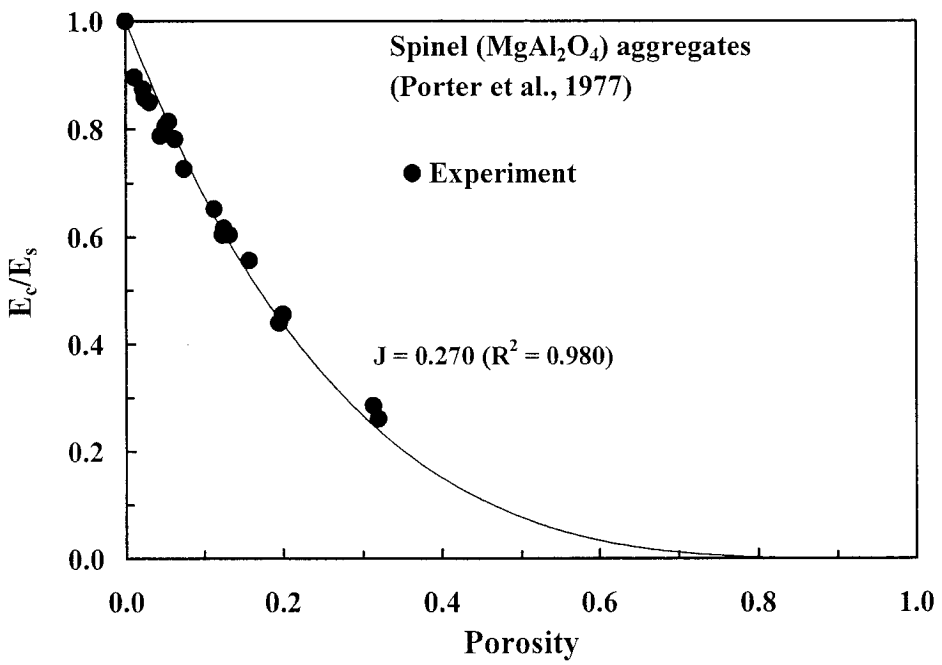

Figure 3.5 Comparison of the theoretical values calculated from the GMR with experimental data on relative Young's modulus of porous material $MgAl_2O_4$ (Porter et al., 1977).

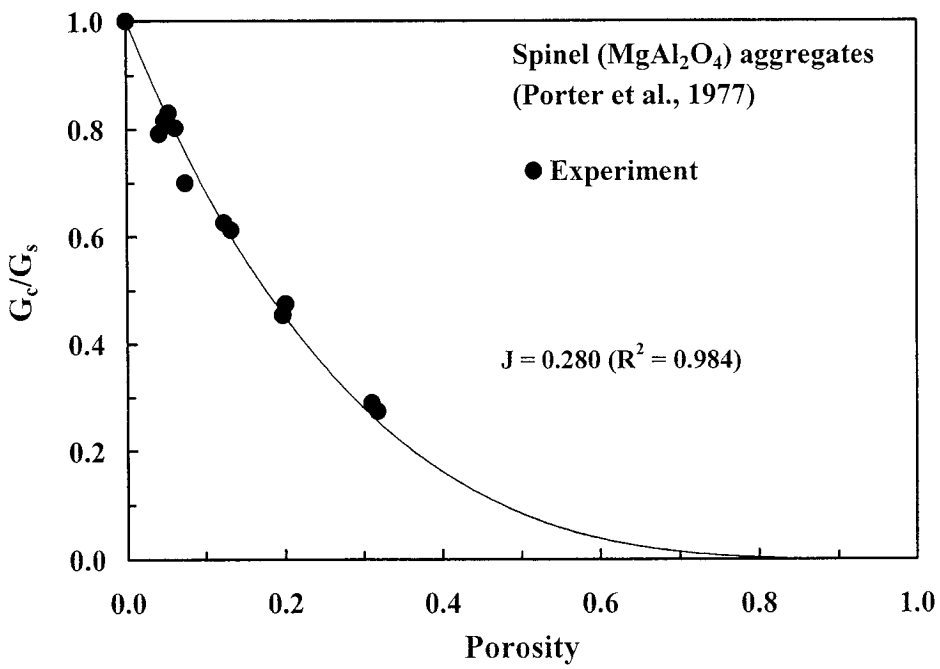

Figure 3.6 Comparison of the theoretical values calculated from the GMR with experimental data on relative shear modulus of porous material $MgAl_2O_4$ (Porter et al., 1977).

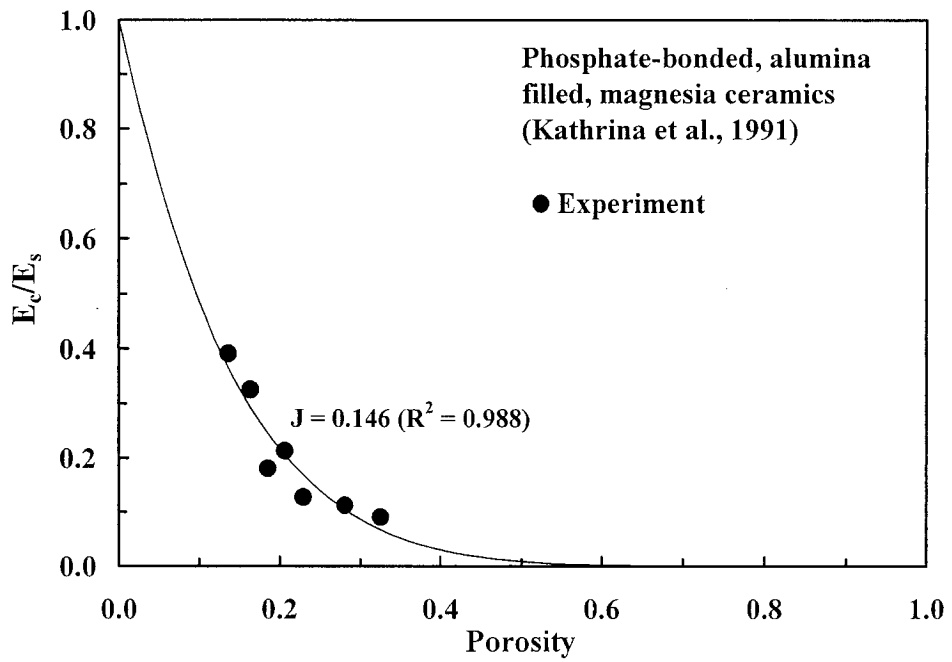

Figure 3.7 Comparison between experimental and theoretical results for relative Young's modulus of phosphate-bonded, alumina filled magnesia ceramics.

Berge et al. (1995) made measurements on P- and S-wave velocities of synthetic sandstone using sintered glass beads with porosities ranging from 1% to 43%. The glass has composition 71-74% by weight SiO_2, 12-15% NaO_2, 8-10% CaO, 1.5-3.8% MgO, 0.2-1.5% Al_2O_3, and 0-0.2% K_2O, and elastic properties K=46.1 GPa, G=29.8 GPa, ρ=2.48 g/cm^3, V_p=5.86 km/s and V_s=3.43 km/s. The overall Young's, bulk and shear moduli of composites were computed from measured densities and acoustic velocities. Figures 3.8 and 3.9 display a clear drop of the relative elastic moduli E_c/E_s and G_c/G_s towards a critical porosity (p_{c1}) of ~0.30. For porosities below ~0.30, the samples have similar microstructures with isolated pores embedded in a continuous solid glass (Berge et al., 1995) and the experimental data can be well described by the GMR (Eq. 2.4) with

J=0.405 and J=0.409 for E and G, respectively. The critical porosity p_{c1} presumably coincides with the minimum porosity for near-closely packed quasi-identical spheres. The J values for E and G decreases progressively from ~0.41 to ~0.25 with increasing porosity from ~0.30 to 0.43, reflecting that the geometry of pores in the synthetic sandstone becomes complex due to the interaction between pores in this range of porosities. For comparison, the Hashin-Shtrikman upper bound (Hashin and Shtrikman, 1963) is equally given in Figures 3.8 and 3.9.

Hashin and Shtrikman (1963) derived the upper and lower bounds on the elastic properties of composite by employing the variational principle that considers the change in strain energy in a loaded homogeneous body due to the insertion of inhomogeneities. In an arbitrary reference cube in the composite which is large compared with the size of the inhomogeneities, yet small compared with the whole body, the volume average of a quantity such as displacement, strain, stress or phase volume fraction is the same for the whole body and the reference cube. The lower bound is obtained from the minimum complementary energy theorem and the upper bound is obtained from the minimum potential energy theorem. Since the Hashin-Shtrikman bounds are considerably narrower than the Voigt and Reuss bounds, they have been widely used for calculating the average elastic moduli of monomineralic aggregates from single crystal elasticity data and calculating the overall elastic moduli and seismic velocities of polyphase aggregates in terms of phase moduli and volume fractions. These bounds are given by the following equations:

$$K_c^U = K_f + \frac{V_m}{\frac{1}{(K_m - K_f)} + \frac{3V_f}{(3K_f + 4G_f)}} \qquad (3.1)$$

$$K_c^L = K_m + \frac{V_f}{\frac{1}{(K_f - K_m)} + \frac{3V_m}{(3K_m + 4G_m)}} \tag{3.2}$$

$$G_c^U = G_f + \frac{V_m}{\frac{1}{(G_m - G_f)} + \frac{6(K_f + 2G_f)V_f}{5G_f(3K_f + 4G_f)}} \tag{3.3}$$

$$G_c^L = G_m + \frac{V_f}{\frac{1}{(G_f - G_m)} + \frac{6(K_m + 2G_m)V_m}{5G_m(3K_m + 4G_m)}} \tag{3.4}$$

where K and G are the bulk modulus and shear modulus, respectively. The superscripts U and L denote the upper and lower bounds, respectively. The Hashin-Shtrikaman bounds on the Young's modulus and Poisson's ratio for the composite can be calculated from the relationships between E, v, K, and G for isotropic and homogeneous materials as given by

$$E = \frac{9KG}{3K + G} \tag{3.5}$$

$$\nu = \frac{3K - 2G}{6K + 2G} \tag{3.6}$$

$$G = \frac{E}{2(1 + \nu)} \tag{3.7}$$

Clearly, the calculations of Hashin-Shtrikman bounds require a full knowledge of bulk and shear moduli and Poisson's ratio of each constituent in the composite. For the GMR

considered in this paper, however, only the values of the modulus (Young's, shear or bulk modulus) and volume fraction of the constituents need to be known.

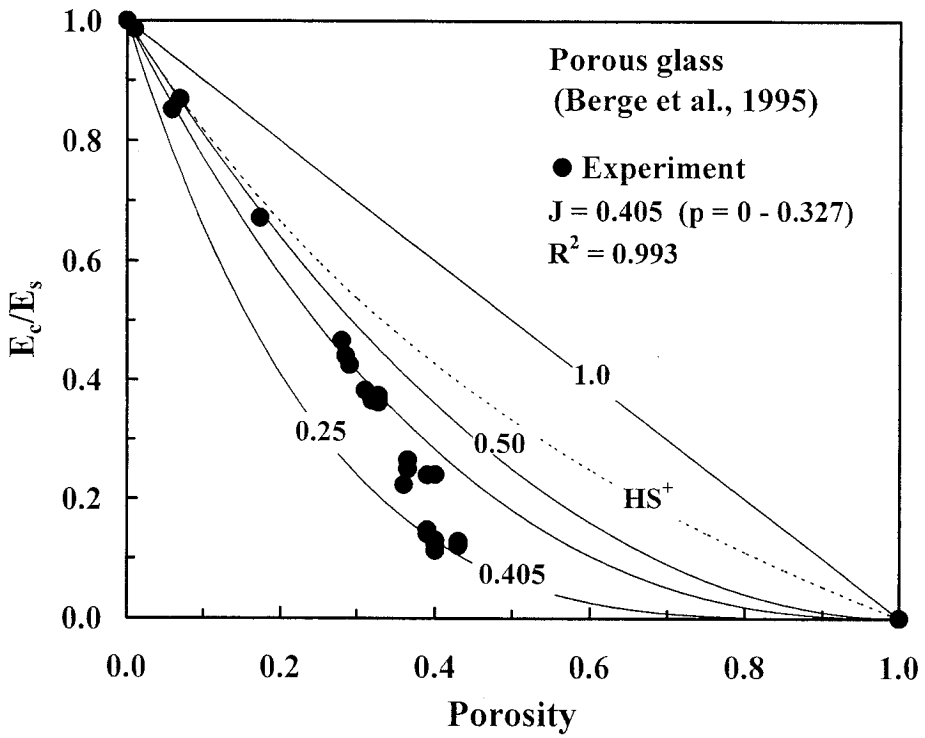

Figure 3.8 Comparison between experimental and theoretical results for relative Young's modulus for sandstone analogs made from fused glass beads. Theoretical curves labeled according to J value. HS+ represents the Hashin-Shtrikman upper bound.

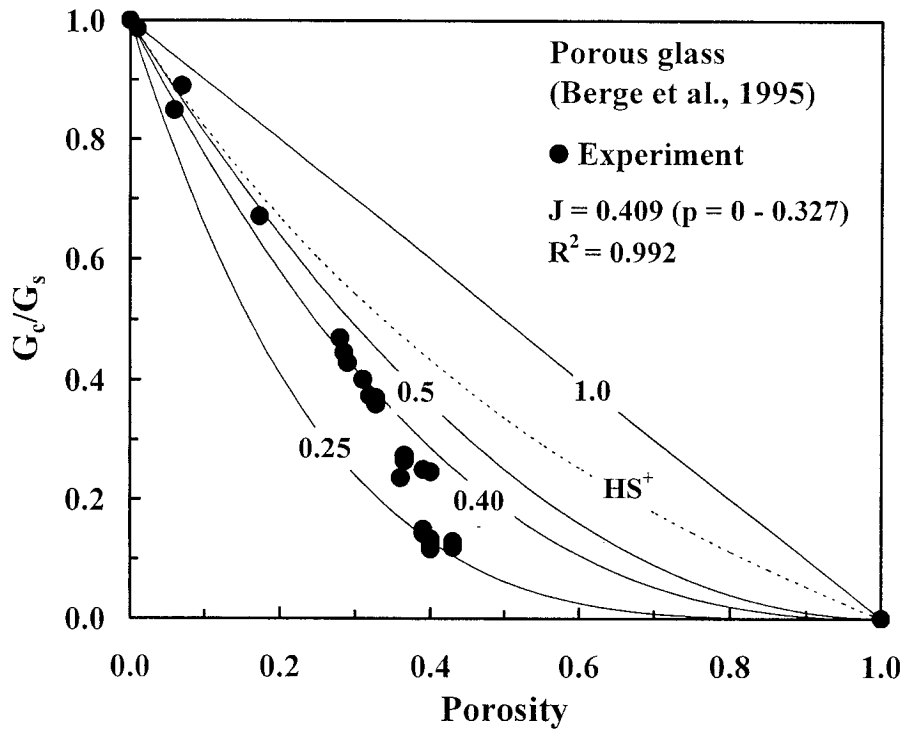

Figure 3.9 Comparison between experimental and theoretical results for relative shear modulus for sandstone analogs made from fused glass beads. Theoretical curves labeled according to J value. HS+ represents the Hashin-Shtrikman upper bound.

Walsh et al. (1965) carried out a series of experiments on the bulk moduli (K) of glass foams over a range of porosities from 0 to 0.7. The glass has the composition (in weight) 54.4% SiO_2, 14.4% B_2O_3, 14.1% CaO, 10% Al_2O_3, 6.5% Na_2O and 0.7% K_2O, K=46 GPa and G=30.5 GPa. Porosity measurements were stated to be accurate ± 0.01. In the samples, the pores are nearly spherical and non-interconnecting (Walsh et al., 1965). Their experimental data are plotted in Fig. 3.10 for comparison with the values calculated from the GMR. The experimental data essentially track the calculated curve with J=0.505 and p_c=1 for samples with $p \leq 0.50$. The Hashin-Shtrikman (Hashin and

Shtrikman, 1963) upper bound (HS^+) overestimates the actual elastic modulus. The Hashin-Shtrikman lower bound (HS^-) is physical meaningless because it results in a zero value for all elastic moduli regardless of porosity. Figure 3.10 shows that the GMR yields a better description than the self-consistent approximation (SC, Budiansky, 1965; Berryman, 1994; Hill, 1965) and the differential method (DM, Berryman, 1994; Cleary, 1980). Further, the exponential expression (Eq. 2.11) is obviously disqualified for describing the data at high porosities.

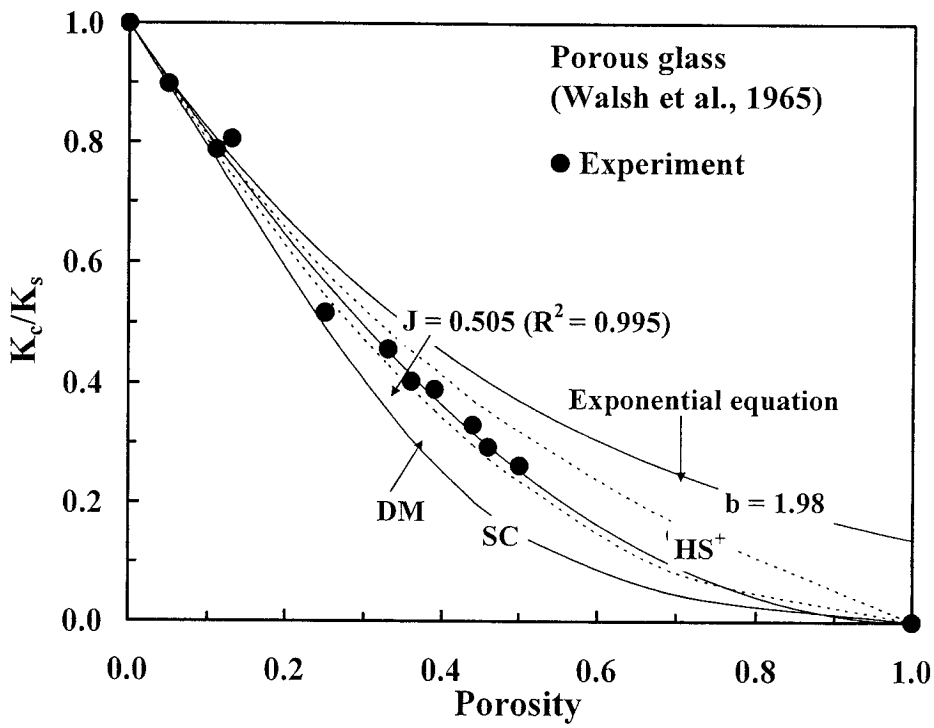

Figure 3.10 Comparison between experimental and theoretical results for relative bulk modulus for glass foams.

Ishai and Cohen (1968) measured the compressive yield strengths of porous epoxy at constant strain rates from 2.25×10^{-2} /s to 4.50×10^{-5} /s. The samples, containing up to 66% porosities, were prepared by whipping the epoxy liquid at different speeds and times according to the desired void ratios. Most of the pores had nearly spherical geometry. Their experimental data except one (Fig. 3.11) are in good agreement with Eq. (2.23) with J=0.513 and p_c=1. The anomaly for a sample with 7% porosity may be due to some errors in the measurement. The experimental data on the compressive strength of Cu/Cu_2O cermets with morphologically complex intergranular pores (Shao et al., 2004) yield a low value of J (J=0.140, Fig. 3.13).

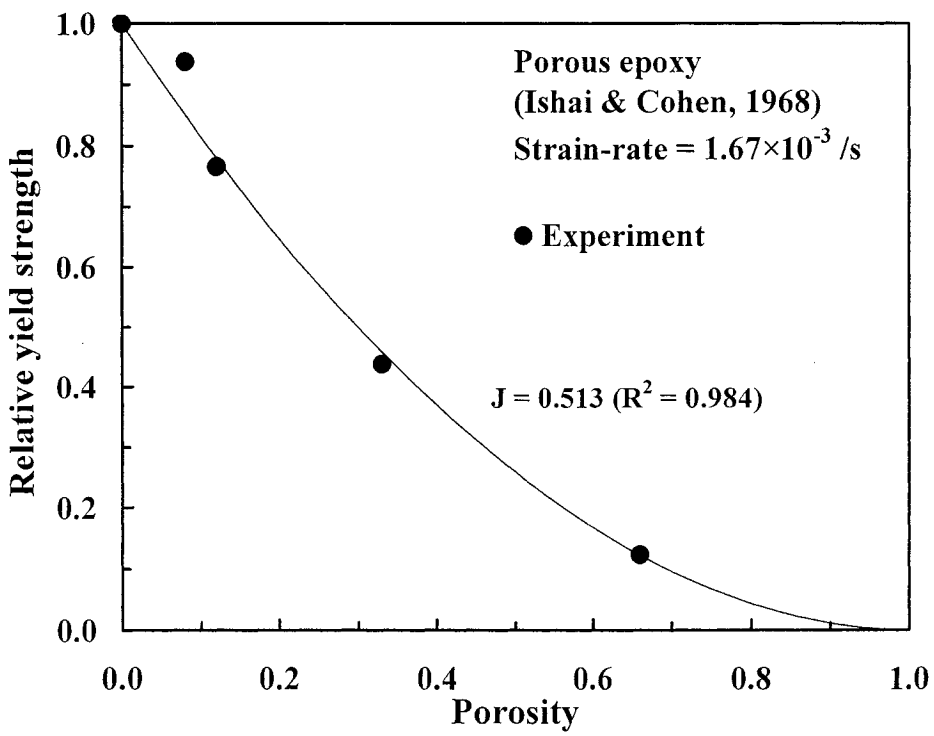

Figure 3.11 Comparison between experimental and theoretical results for relative yield strength of porous epoxy.

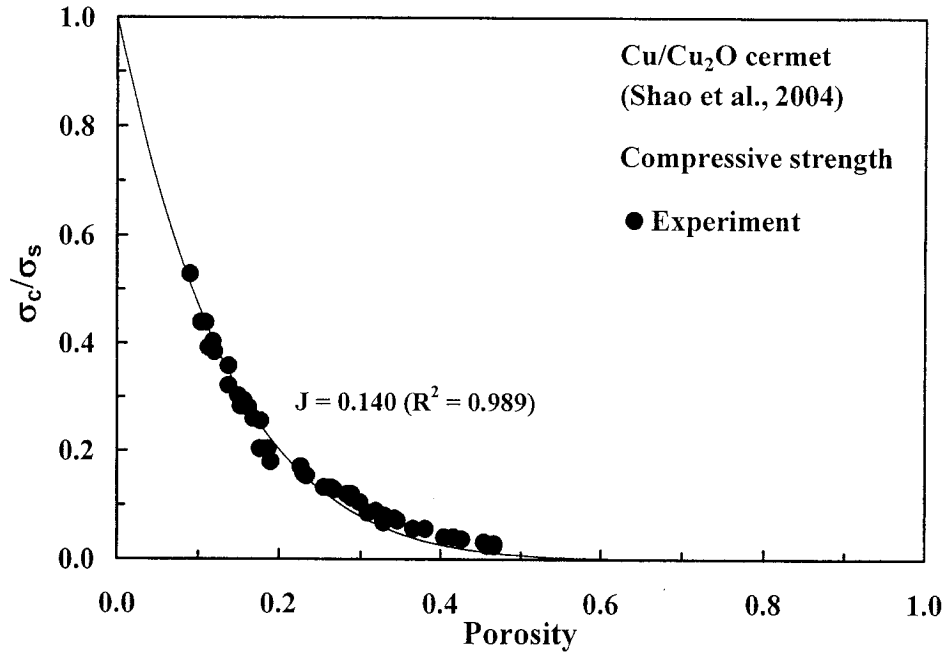

Figure 3.12 Comparison between experimental and theoretical results for relative compressive strengths for Cu/Cu_2O cermets.

Interestingly, Figures 3.10, 3.11 and 3.12 display a clear effect of pore geometry on the mechanical properties of solid materials. Isolated spherical pores (Figs. 3.10 and 3.11) cause the J value to be higher than shaped-cornered holes and flat elliptical cavities (Fig. 3.12; also see Fig. 3.7). The value of $J \approx 0.5$ for porous glass (Walsh et al., 1965) and epoxy (Ishai and Cohen, 1968) is consistent with the theoretical prediction (Boccacini et al., 1995) for solids containing isolated spherical pores.

The above comparison between calculation and experiment yields consistently $p_c=1$. This indicates that the effective mechanical properties does not vanish unless $p=1$. This

is also consistent with a fact that it is possible to fabricate ceramics with a porosity as high as 0.98 (Gibson and Ashby, 1988). This implies that the solid medium in the samples form a continuous stress-supporting framework although the pores can be interconnected. Therefore, Eq. (2.23) is exactly identical to Eq. (2.4), the latter is derived directly from the GMR, for the materials with p_c=1.

Figures 3.13-3.17 demonstrate the relationship between ductile flow strength and porosity for sintered powder metal compacts such iron, cooper, aluminum, nickel and their alloys (Beiss and Dalgic, 2001; Weaver et al., 1972; Krantz, 1969; German, 1977). Up to a porosity p = ~0.25, the strength of samples can be well described by the GMR (Eq. 2.4) with J=~0.25. For higher porosities (p>~0.25), however, the J value to fit the experimental data decreases progressively with increasing porosity. Although no detailed information about the actual pore shape at different porosity levels is available from the original literature, it is likely that the loss of isolation of the pores occurs at p> ~0.25. The pores change from being isolated, closed and sharp-cornered to interconnected channel pores.

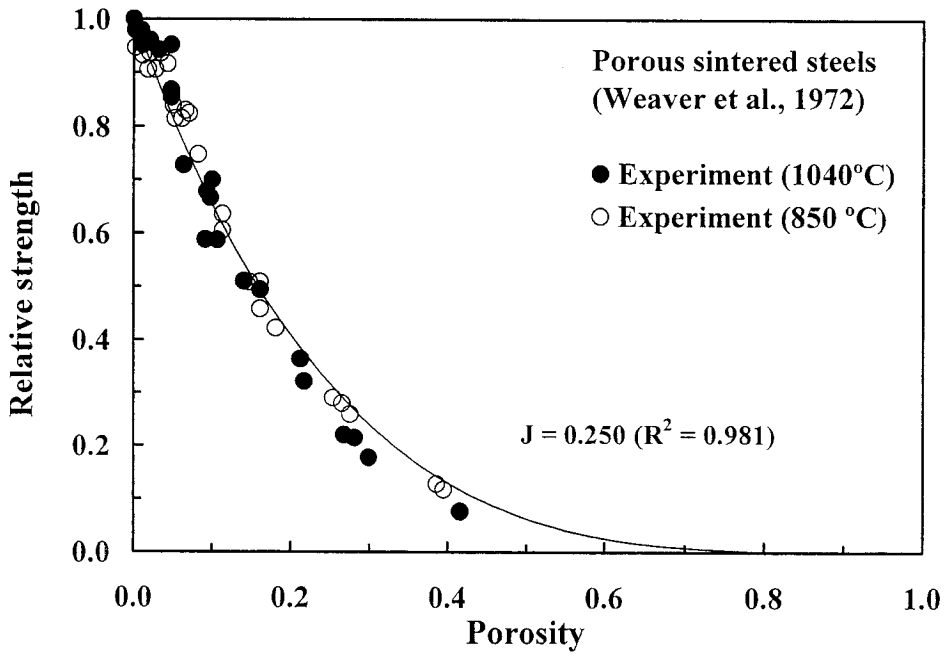

Figure 3.13 Relative ductile strength for Fe aggregates plotted against porosity.

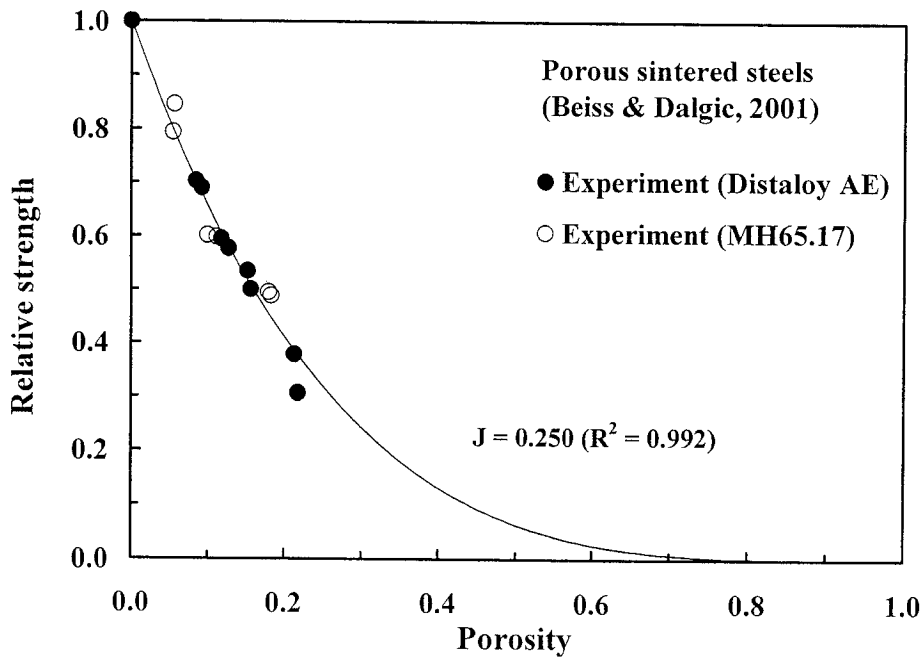

Figure 3.14 Relative ductile strength for sintered steels plotted against porosity.

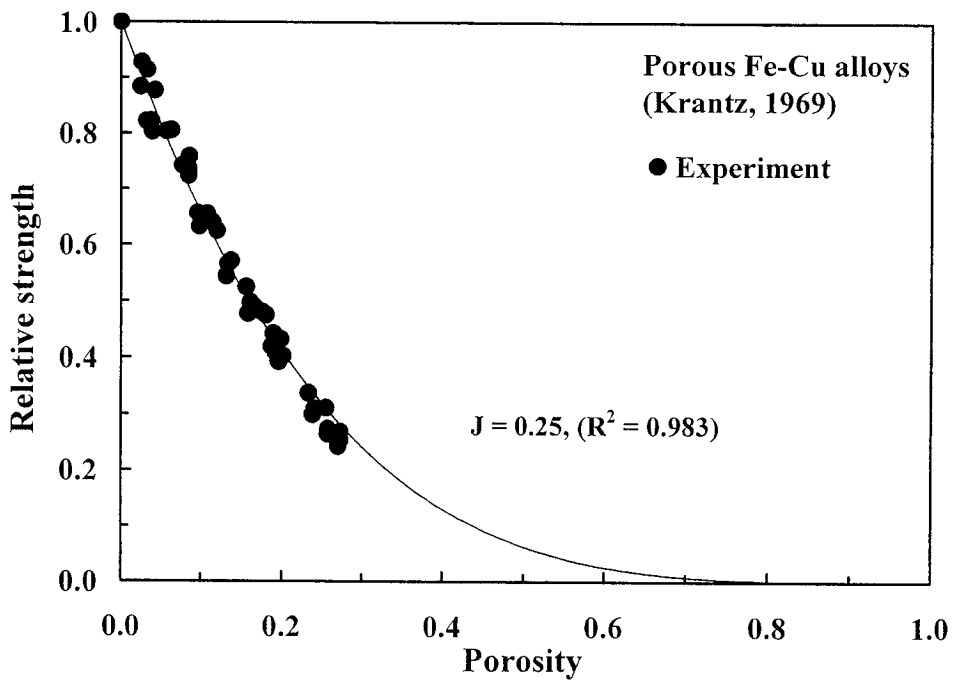

Figure 3.15 Relative ductile strength for Fe-Cu alloys plotted against porosity.

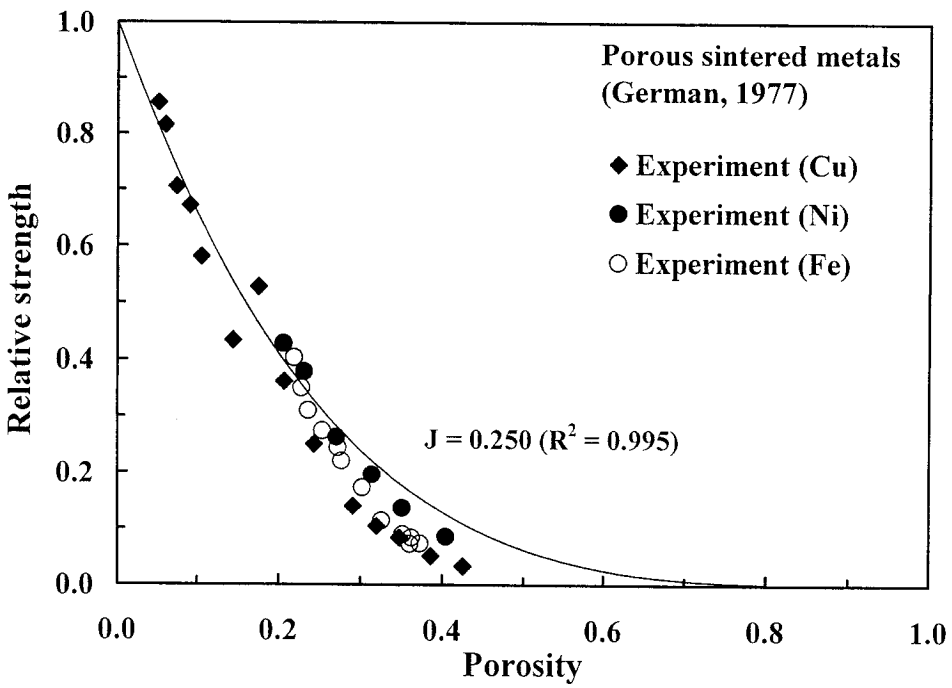

Figure 3.16 Relative ductile strength for sintered Cu, Ni and Fe plotted against porosity. The labeled J value is obtained by fitting the experimental data (p<0.26) with the GMR.

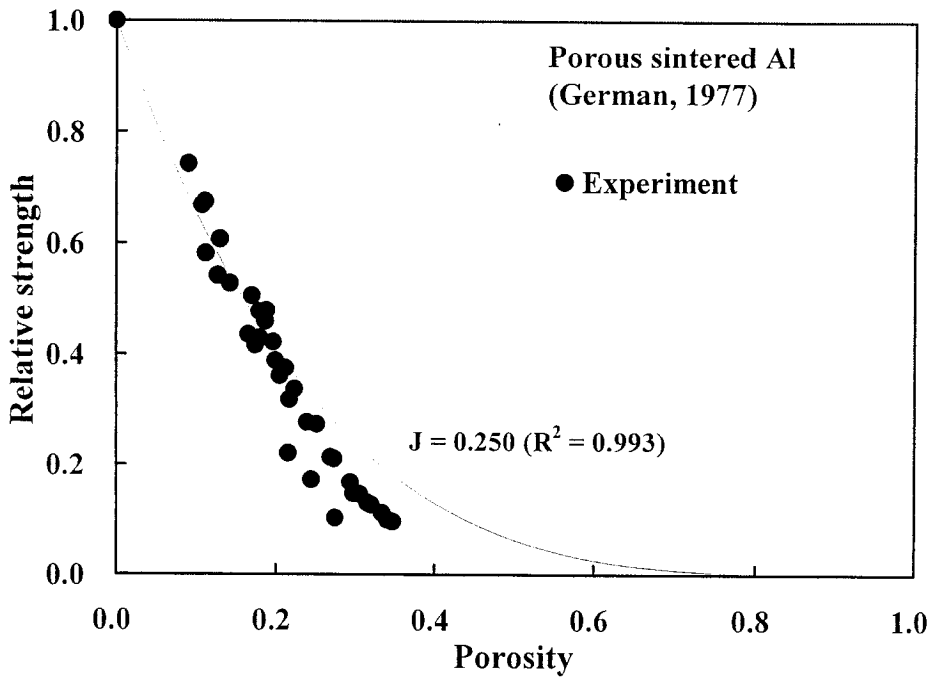

Figure 3.17 Relative ductile strength for sintered Al plotted against porosity. The labeled J value is obtained by fitting the experimental data (p<0.26) with the GMR.

Using an ultrasonic technique, Matikas et al. (1997) measured the longitudinal (P-wave) and shear (S-wave) acoustic velocities (V_p and V_s) and then calculated the Young's, shear and bulk moduli as well as the Poisson's ratio for porous titanium aluminide compacts. The relative elastic properties as a function of porosity are plotted in Fig. 3.18. J=0.531 and J=0.385 for V_p and V_s, respectively. For the same set of samples, J values needed to best fit the experimental data are different for different elastic properties: J=0.550, 0.248, 0.227 and 0.134 for the Poisson's ratio (υ), shear modulus (G), Young's modulus (E) and bulk modulus (K), respectively. This aspect should receive a further detailed study.

Figure 3.19 illustrates a general trend of the variation in the P- and S-wave velocities (V_p and V_s) in water-saturated basalts at a confining pressure of 200 MPa (Ji et al., 2002). The results are of geological interests because the oceanic crust is compositionally dominated by the basalts. The pores are filled with water in which V_p=1.5 km/s and V_s=0 km/s. The theoretical curves for V_p and V_s were calculated according to Eq. (2.1) and Eq. (2.4), respectively. The GMR with J=0.235 and J=0.214 provides statistically meaningful descriptions for the V_p and V_s data, respectively. Scatter in the velocity data plots can be attributed to variations in shape, size, and spatial distributions and orientations of pores within the natural basaltic samples.

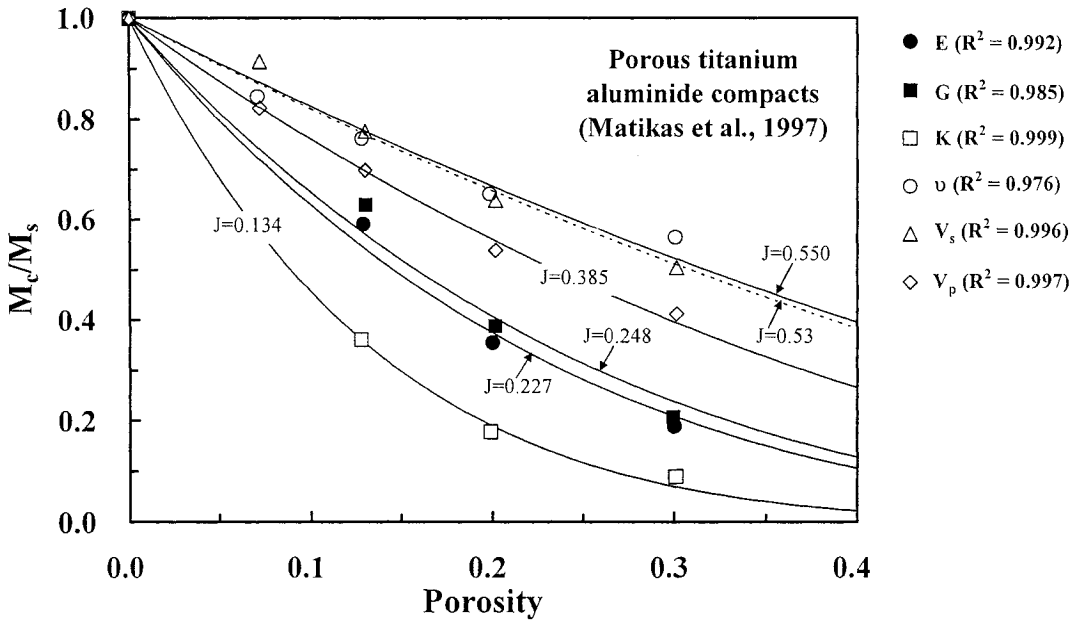

Figure 3.18 Relative elastic properties (*E, G, K*, υ, V_p and V_s) for titanium aluminide (Ti-24Al-11Nb) compacts plotted against porosity.

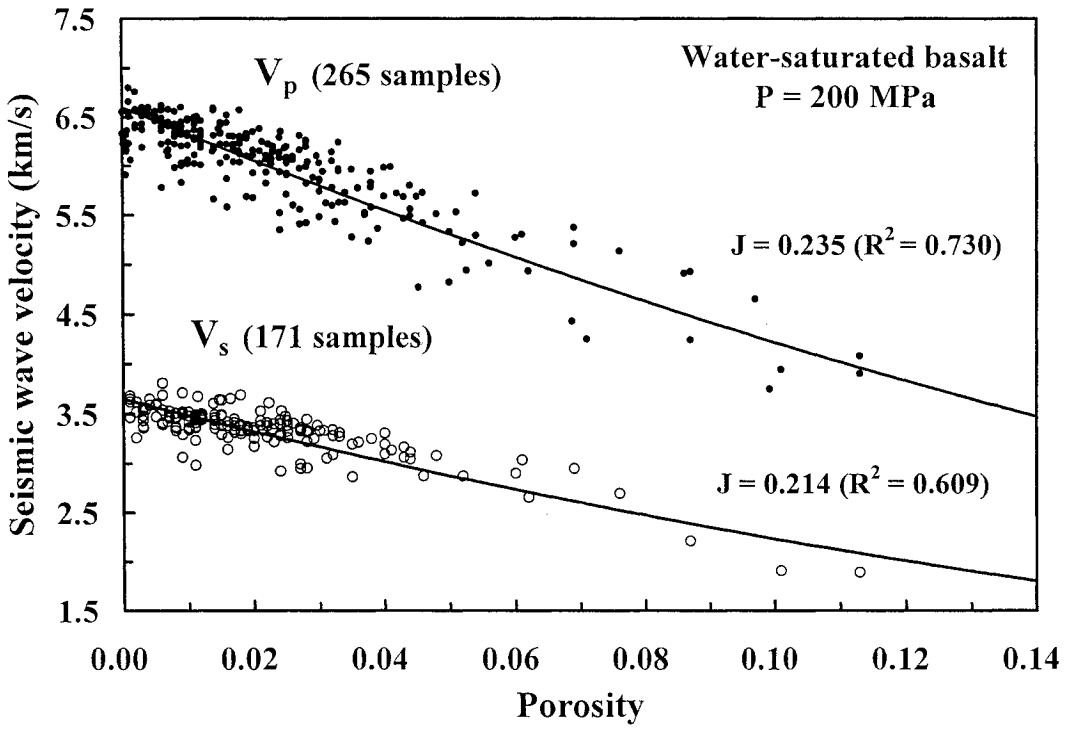

Figure 3.19 P-wave and S-wave velocities (km/s) in water-saturated basalts plotted against porosity.

Chapter 4. Conclusions

The major conclusions from the present investigation are summarized below:

The generalized mixture rule (GMR) is a rigorous mathematical formula of simple symmetry. It postulates no assumption on either physical properties or processes (or microstructures). Thus, it is reasonable to believe that the GMR reflects the random nature of microstructure in polyphase materials such as crystalline rocks.

The GMR provides a unified description for the best fitting relationship between the overall mechanical properties (e.g., elastic moduli, yield and flow strengths) and the volume fraction and microstructure of each component in multiphase composites. For porous solids, various well-known equations such as Balshin power law (Balshin, 1949), Duckworth exponential equation (Duckworth, 1951), Gibson-Ashby formula (Gibson and Ashby, 1988), and Phani expression (Phani, 1986) on the relationship between the mechanical properties and porosity can be derived directly from the GMR. For porosities <30%, the GMR is consistent with the results of previous theoretical models based on some idealized uniform structures [e.g., Eudier (1962), Ramakrishnan and Arunachalam (1990), Ishai and Cohen (1967), and Rice (1998)] within an error of no more than a few percent. Further, the agreement between the GMR and extensive experimental data on a wide range of polyphase systems including porous solids could not be considered to be fortuitous. The GMR should have some physical validity as a theory or at least a hypothesis or a phenomenological tool for a general description of the mechanical properties of multiphase materials including porous solids. Rigorous theoretical analyses, which could be a very challenging topic of mathematic mechanics, are definitively needed because the fundamental physical meaning of the GMR has not

been clear. The present work thus provides a foundation upon which to base further studies.

The characteristic exponent J of the GMR provides a scaling parameter for quantitatively describing the effects of complex microstructures on the overall physical properties. This parameter, which is named the microstructural coefficient (Ji, 2004a and b), is controlled mainly by the shape, size distribution, continuity and connectivity of the phases, and may reflect the formation processes of the material. Thus, the J value can be used to classify polyphase materials. For lotus-type porous materials with long cylindrical or hexagonal pores oriented parallel and perpendicular to the stress direction, J=1 and J=1/3, respectively. $J\rightarrow 0$ (the geometrical mean), which is equivalent to the Hashin-Shtrikman lower bound (Hashin and Shtrikman, 1963) in the case of porous materials), represents an extreme case where the effective property of a porous material will vanish, regardless of porosity. J=~0.50 for porous materials in which isolate, perfectly spherical pores are embedded randomly in a continuous solid matrix. For the Young's modulus, J=~0.25 for polycrystalline materials containing shaped-cornered holes. The presence of flat elliptical cavities will result in a smaller value of J. Generally, intergranular, continuous, channel pores or cavities cause a lower J value than intragranular, isolated and rounded pores. Hence, rounding and disconnecting the pores should result in an increase in the effective mechanical properties of materials with a constant porosity. In other words, optimizing the overall mechanical properties of materials can be done through introducing different volume fractions and/or different shapes of pores into the solids. An additional finding is that the values of J for shear, Young's, shear and bulk moduli and Poisson's ratio may not be identical even for a porous material with a constant microstructure. Hence, there is a need for further careful investigation on this subject particularly for Earth materials.

The application of the GMR to predict the overall properties of polyphase materials is more direct compared with other approaches such as Hashin-Shtrikman upper and

lower bounds (Hashin and Shtrikman, 1963). In the case of elasticity, the GMR does not need to know bulk or shear moduli separately. However, the calculations of Hashin-Shtrikman bounds require full information on the bulk and shear moduli of each phase of the materials. A full set of elastic data is usually lacking because only one elastic property is often measured. In the latter cases, the Hashin-Shtrikman bounds cannot be calculated. For porous materials, the Hashin-Shtrikman upper and lower bounds lie too far apart to be useful in predicting elastic properties as a function of porosity because the pores have a null strength and the Hashin and Shtrikman lower bound is always zero for all moduli regardless of the porosity.

The GMR, compared with many complicated numerical modeling methods that are tedious to employ for each composite, has a particular advantage to have an analytical formula rather than a computational one. This obvious advantage is extremely useful if it is desired to invert the mechanical data of a composite to calibrate the microstructure or to estimate the property or the volume fraction of an end-member component. Thus, the GMR should be readily used into modeling the flow strengths of polymineralic rocks deformed under various physical and chemical conditions (e.g., temperature, pressure, strain rate and water content) in the lithosphere.

REFERENCES

ALLEN, J.R.L., 1984. Packing of sedimentary particles. In: Allen, J.R.L., Sedimentary Structures: Their character and physical basis. Elsevier, Amsterdam, P. 137-177.

ARGOITIA, A., BAUMARD, J.F., GAULT, C. 1987. in "High tech ceramics", edited by Vincenzini, P. (Elsevier Science Publishers B.V., Amsterdam, The Netherlands). P. 1381.

BALSHIN, M.Y. 1949. "Relation of mechanical properties of powder metals and their porosity and the ultimate properties of porous metal-ceramic materials", *Dokl. Akad. Nauk. (SSSR)*, 67:5. 831-834.

BEISS, P.,DALGIC, M. 2001. "Structure property relationships in porous sintered steels". *Materials Chemistry and Physics*. 67. 37-42.

BERGE, P.A., BONNER, B.P., BERRYMAN, J.G. 1995. "Ultrasonic velocity-porosity relationships for sandstone analogs made from fused glass beads". *Geophysics*. 60. 108-119.

BERRYMAN, J.G. 1994. "Role of porosity in estimates of composite elastic constants". *Journal of Energy Resources Technology*. 116. 87-96.

BIDDULPH, R.B., June 1972. "Rupture strength and Young's modulus as functions of porosity in polycrystalline magnesium oxide " M.Sc. Thesis, Department of Ceramic Engineering, University of Utah.

BLANKS, K.S., KRISTOFFERSSON, A., CARLSTROM, E., CLEGG, W. J. 1998. "Crack deflection in ceramic laminates using porous interlayers". *Journal of the European Ceramic Society*. 8. 1945-1951.

BOCCACINI, A.R., ONDRACEK, G. AND MOMBELLO, E. (1995) *Journal of Materials Science Letters*. 14, 534.

BOCH, P., GLANDUS, J.C. 1979. "Elastic properties of silicon oxynitride". *Journal of the American Ceramic Society*. 14. 379-385.

BOOCOCK, J., FURZER, A.S., MATTHEWS, J.R. 1972. Report: AERE-M2565, Process Technology Division, Atomic Energy Research Establishment, Harwell, Berkshire, England

BUDIANSKY, B. 1965. "On the elastic moduli of some heterogeneous materials". *Journal of the Mechanics and Physics of Solids*. 13. 223-227.

CARNAHAN, R.D. 1968. "Elastic properties of silicon carbide". *Journal of the American Ceramic Society*. 51. 223-224.

CHAMPAGNE, B., ANGERS, R. 1979. "Mechanical properties of hot-pressed B-B_4C materials". *Journal of the American Ceramic Society*. 62. 149-153.

CHANDLER, B.A., DUDERSTADT, E.C., WHITE, J.F. 1963. "Fabrication and properties of extruded and sintered BeO". *Journal of nuclear materials*. 8. 329-347.

CHU, C., BAR, K., SINGH, J.P., LORETTA, K.C., GILLONE, M.C., POEPPEL, R.P., ROUTFORT, J.L. 1989. "Mechanical properties of polycrystalline lithium orthosilicate". *Journal of the American Ceramic Society*. 72. 1643-1648.

CLEARY, M.P., CHEN, I.W., LEE, S.M. 1980. "Self-consistent techniques for heterogeneous media". *Journal of Engineering Mechanics*. 106. 861-887.

COBLE, R.L., KINGERY, W.D. 1956. "Effect of porosity on physical properties of alumina". *Journal of the American Ceramic Society*. 39. 377-385.

DATTA, S.K., MUKHOPADHYAY, A.K., CHAKRABORTY, D. 1989. "Young's modulus-porosity relationships for Si_3O_4 ceramics-a critical evaluation". *American Ceramic Society bulletin*. 48. 2098.

DEPORTU, G., VINCENZINI, P. 1980. "Young's modulus of silicon nitride hot pressed with ceria additions". *Ceramurgia International*. 6. 129-132.

DOLE, S.L., HUNTER, O., CALDERWOOD, F.W. 1977. "Elastic properties of polycrystalline scandium and thulium sesquioxide". *Journal of the American Ceramic Society*. 60. 167-168.

DUCKWORTH, W.H. 1951. "Precise tensile properties of ceramic bodies'. *Journal of The American Ceramic Society*. 34, 1-9.

EINSTEIN, A.E. 1906. " Eine neue bestimmung der molekuldimensionen". *Ann. Phys. Lpz.* 19. 289-306.

EUDIER, M. 1962. "The mechanical properties of sintered low-alloy steels". *Powder Metallurgy*. 9. 278-290.

FRYXELL, R.E., CHANDLER, B.A. 1964. "Creep, strength, expansion, and elastic moduli of sintered BeO as a function grain size, porosity, and grain orientation". *Journal of the American Ceramic Society*. 47. 283-291.

GENT, A.N., THOMAS, A.G. 1959. "The Deformation of Foamed Elastic Materials". *Journal of Applied Polymer Science*. 1. 107-113.

GERMAN, R.M. 1977. "Strength dependence on porosity for P/M compacts". *International Journal of Powder Metallurgy & Powder Technology*. 13. 259-265.

GIBSON, L.J., ASHBY, M.F. 1982. "The mechanics of three-dimensional cellular materials". *Proceedings of the Royal Society of London*. A382, 43-59.

GIBSON, L.J., ASHBY, M.F. 1988. "The mechanics of three-dimensional cellular materials". *Cellular Solids: Structure & Properties*. Pergamon. Oxford.

GRIFFITHS, T. J., DAVIES, R., BASSETT, M.B. 1979. "Analytical study of effects of pore geometry on tensile strength of porous materials". *Powder Metallurgy*. 3. 119-123.

HAGLUND, J.A., HUNTER, O. 1973. "Elastic properties of polycrystalline monoclinic Gd_2O_3". *Journal of the American Ceramic Society*. 56. 327-330.

HASHIN, Z. 1968. "Elasticity of ceramic systems". in R. M. Fulrath, J. A. Pask (Eds.), *Ceramic microstructures*. John Wiley and Sons, New York. 313.

HASHIN, Z., SHTRIKMAN, S. 1963. "A variational approach to the elastic behaviour of multiphase materials". *Journal of the Mechanics and Physics of Solids*. 11. 127-140.

HASSELMAN, D.P. 1962. "On the porosity dependence of the elastic moduli of polycrystalline refractory materials". *Journal of the American Ceramic Society*. 45. 452-453.

HAYNES, R. 1971. "Effect of porosity content on the tensile strength of porous materials". *Powder Metallurgy*. 14. 64-70.

HILL, R. 1965. "A self-consistent mechanics of composite materials". *Journal of the Mechanics and Physics of Solids*. 13. 213-222.

HUNTER, O., GRADDY, G.E. 1976. "Porosity Dependence of Elastic Properties of Polycrystalline Lu_2O_3". *Journal of the American Ceramic Society*. **59**(1-2). 82.

HUNTER, O., KORKLAN, H.J., SUCHOMEL, R.R. 1974. "Elastic Properties of Polycrystalline Monoclinic Sm_2O_3". *Journal of the American Ceramic Society*. **57**(6). 267-268.

HYUN, S.K., MURAKAMI, K., NAKAJIMA, H. 2001. " Anisotropic mechanical properties of porous copper fabricated by unidirectional solidification". *Materials Science and Engineering*. A299, 241-248.

ICHITSUBO, T., TANE, M., OGI, H., HIRAO, M., IKEDA, T., NAKAJIMA, H. 2002. "Anisotropic elastic constants of lotus-type porous copper: measurements and micromechanics modeling". *Acta materialia*. 50. 4105-4115.

ISHAI, O. AND COHEN, L.J. 1967. "Elastic properties of filled and porous epoxy composites". *International Journal of Mechanical Sciences*. 9. 539-546.

ISHAI, O., COHEN, L.J. 1968. "Effect of fillers and voids on comprehensive yield of epoxy composites". *Journal of Composite Materials*. 2. 302-315.

JANOWSKI, K.R., ROSSI, R.C. 1968. "Mechanical degradation of MgO by water vapor". *Journal of the American Ceramic Society*. 51. 453-455.

JI, S. 2004a. "A generalized mixture rule for estimating the viscosity of solid-liquid suspensions and mechanical properties of polyphase rocks and composite materials" *Journal Geophysic Research*. 109, doi: 10.1029/2004JB003124.

JI, S. 2004b. "Generalized means as an approach for predicting the Young's modulus of multiphase materials". *Materials Science and Engineering*. A366. 195-201.

JI, S., WANG, Q., XIA, B. 2002. *Handbook of Seismic Properties of Minerals, Rocks and Ores*. Polytechnic International Press. Montreal.

KATHRINA, T., ROUND, R., BRIDGE, B. 1991. "An investigation of the composition dependence of the elasticity, reaction rate and porosity of orthophosphate bonded ceramics using an ultrasonic double-probe method". *Journal of Physics. D, Applied Physics*. 24. 1673-1686.

KNUDSEN, F.P. 1959. "Dependence of mechanical strength of brittle polycrystalline specimens on porosity and grain size". *Journal of the American Ceramic Society*. 42. 376-387.

KNUDSEN, F.P. 1962. "Effect of Porosity on Young's Modulus of Alumina". *Journal of the American Ceramic Society*. 45. 94-95.

KOVACIK, J. 1999. "Correlation between Young's modulus and porosity in porous materials". *Journal of Materials Science Letters*. 13. 1007-1010.

KRANTZ, T. 1969. "Effect of density and composition on the dimensional stability and strength of iron-copper alloys". *International Journal of Powder Metallurgy*. 5. 35-43.

LEDERMAN, J. M. 1971. "The prediction of the tensile properties of flexible foams". *Journal of Applied Polymer Science*. 15. 693-703.

LIEBLING, R.S. 1967. "Effect of low porosity on the elastic properties of boron carbide". *Journal of the American Ceramic Society*. 2. 1035-1040.

MANNING, W.R., HUNTER, O. 1969. "Elastic Properties of Polycrystalline Yttrium Oxide, Dysprosium Oxide, Holmium Oxide, and Erbium Oxide: Room Temperature Measurements". *Journal of the American Ceramic Society*. 52. 436-442.

MARLOWE, M.O., WILDER, D.R. 1965. "Elasticity and internal friction of polycrystalline yttrium oxide". *Journal of the American Ceramic Society*. 48. 227-233.

MATIKAS, T.E., KARPUR, P., SHAMASUNDAR, S. 1997. "Measurement of the dynamic elastic moduli of porous titanium aluminide compacts". *Journal of materials science*. 32. 1099-1103.

MCLAUGHLIN, R. 1977. "A study of the differential scheme for composite materials". *International journal of engineering science*. 15. 237-244.

NEUBER, H. and WIMMER, A. March 1968. Technical Report AFMLTR-68-23, Air Force Materials Laboratory, Wright-Patter-son Air Force Base, OH.

NIELSEN, L.F. 1982. "Elastic properties of two-phase materials". *Materials science and engineering*. 52. 39-62.

NORRIS, A.N. 1985. "A differential scheme for the effective moduli of composites". *Mechanics of Materials*. 4. 1-16.

PANAKKAL, J.P., GHOSH, J.K. 1984. "Ultrasonic velocity in sintered uranium dioxide pellets". *Journal of the American Ceramic Society*. 3. 835-836.

PAUL, B. 1960. "Prediction of elastic constants of multiphase materials". *Transactions of Metallurgical Society, AIME*. 218. 36-41.

PETRAK, D.R., RANKIN, D.T., RUH, R., SISSON, R.D. 1975. "Effect of porosity on the elastic moduli of CoO, CoO-MgO solid solutions, and $CoAl_2O_4$". *Journal of the American Ceramic Society*. 58. 78-80.

PHANI, K.K. 1986. "Young's modulus-porosity relation in gypsum systems". *American Ceramic Society Bulletin*. 65. 1584-1586.

PORTER, D.F., REED, J.S., LEWIS III, D. 1977. "Elastic moduli of refractory spinels". *Journal of the American Ceramic Society*. 60. 345-349.

RAMAKRISHNAN, N., ARUNACHALAM, V.S. 1990. "Effective elastic moduli of porous solids" *Journal of Materials Science*. 25. 3930-3937.

RAMAKRISHNAN, N., ARUNACHALAM, V.S. 1993. "Effective elastic moduli of ceramic materials". *Journal of the American Ceramic Society*. 76. 2745-2752.

REYNAUD, C., THEVENOT, F., CHARTIER, T., BESSON, J.L. 2005 "Mechanical properties and mechanical behaviour of SiC dense-porous laminates". *Journal of the European Ceramic Society*. 25. 589-597.

REYNAUD, C., THEVENOT, F. 2000. "Porosity dependence of mechanical properties of porous sintered SiC: Verification of the minimum solid area model". *Journal of Materials Science Letters*. 19. 871-874.

RICE, R.W. 1977. "Microstructure dependence of mechanical behavior of ceramics". *Treatise on Materials Science and Technology-Properties and Microstructures*, Academic Press. New York. 11. P. 199-381.

RICE, R.W. 1997. "Limitations of pore-stress concentrations on the mechanical properties of porous materials". *Journal of materials science*. 32. 4731-4736.

RICE, R.W. 1998. "Evaluation of the porosity dependence of properties". *Porosity of Ceramics*, Marcel Dekker Inc. New York. P. 43-99.

ROGERS, C.D.F., DIJKSTRA, T.A., SMALLEY, I.J. 1994. Particle packing from an Earth science viewpoint. Earth-Science Review 36, 59-82.

ROSCOE, R. 1952. "The viscosity of suspensions of rigid spheres". *British journal of Applied Physics*. 3. 367-369.

ROSSI, R. 1968. "Prediction of the elastic moduli of composites". *Journal of the American Ceramic Society*. 51. 433-439.

RUSS, J.C. 1986. *Practical Stereology*. Plenum Press. New York.

SCHREIBER, E. 1968. "Comment on the elastic modulus-porosity relation". *Journal of the American Ceramic Society*. 51. 541-542.

SHAO, W.Z., IVANOV, V.V., ZHEN, L., CUI, Y.S., YANG, D.Z. 2004. "Effect of porosity and cooper content on compressive strength of Cu/Cu_2O cermet". *Journal of materials science*. 39. 731-732.

SMITH, D.F., CRANDALL, W.B. 1964. "Calculated high-temperature elastic constants for zero porosity monoclinic zirconia". *Journal of the American Ceramic Society*. 47. 624-627.

SOROKA, I., SEREDA, P.J. 1968. "Interrelation of hardness, modulus of elasticity, and porosity in various gypsum systems". *Journal of the American Ceramic Society* 51. 337-340.

SPRIGGS, R.M. 1961. "Expression for effect of porosity on elastic modulus of polycrystalline refractory materials, particularly aluminium oxide". *Journal of the American Ceramic Society*. 44. 628-629.

SPRIGGS, R.M., BRISSETTE, L.A., VASILOS, T. 1962. "Expressions for shear modulus and poisson's ratio of porous refractory oxides". *Journal of the American Ceramic Society*. 45. 198-199.

STAUFFER, D., AHARONY, A. 1992 *Introduction to Percolation Theory*, Taylor & Francis, London.

WAGH, A.S., POEPPEL, R.B., SINGH, J.P. 1991. "Open pore description of mechanical properties of ceramics". *Journal of materials science*. 26. 3862-3868.

WALSH, J.B., BRACE, W.F., ENGLAND, A.W. 1965. "Effect of Porosity on Compressibility of Glass". *Journal of the American Ceramic Society*. 48. 605-608.

WANG, J.C. 1984. "Young's modulus of porous materials". *Journal of materials science*. 19. 809-814.

WEAVER, C.H., BUTTERS, R.G., LUND, J.A. 1972. "Hot rolling behaviour of iron powder performs" *International journal of powder metallurgy*. 8. 3-15.

WONG, P., KOPLIK, J., TOMANIC, J.P. 1984. "Conductivity and permeability of rocks" *Physical review*. B30. 6606-6614.

ZIMMERMAN, W. 1991. "Elastic moduli of a solid containing spherical inclusions". *Mechanics of Materials*. 12. 17-24.